THE UNIVERSITY OF MICHIGAN
INDUSTRY PROGRAM OF THE COLLEGE OF ENGINEERING

OBSERVATION OF THE ASSOCIATED PRODUCTION OF STRANGE PARTICLES PRODUCED BY POSITIVE PI MESONS

John C. Vander Velde

December, 1957

IP-251

Doctoral Committee:

Professor Donald A. Glaser, Chairman
Professor Robert C. F. Bartels
Professor Wayne E. Hazen
Associate Professor Robert W. Pidd
Professor George E. Uhlenbeck

PREFACE

In any high energy physics experiment of the present type there are necessarily many people who contribute to its success. We would, therefore, like to acknowledge our indebtedness and express our sincerest thanks as follows:

To Professor D. A. Glaser, who suggested the problem, for his constant encouragement and generous help throughout its completion.

To John L. Brown for his major share in building and operating the equipment and for many helpful discussions during the analysis.

To Professors D. I. Meyer and M. L. Perl for their assistance in organizing and performing the experiment.

To the staff at Brookhaven National Laboratory for their kind hospitality and aid during my stay there. In particular, to Dr. J. W. Cronin, who was instrumental in designing the beam set-up, performed all the counter measurements, and was very helpful during his stay at Michigan in the early stages of the analysis. Also to Dr. D. C. Rahm whose design and operation of the rapid beam ejector contributed much to the success of the experiment.

To R. Hartung for his untiring efforts in programing and operating the University's I.B.M. 650 Computer.

To Elsie M. Brown and Sharlene Nelson for their cheerful assistance in scanning the pictures.

This work was supported in part by the United States Atomic Energy Commission.

TABLE OF CONTENTS

LIST OF FIGURES

LIST OF TABLES

INTRODUCTION

During the few years that have elapsed since the first identification of strange particles,[1] a great deal of effort has gone into the further elucidation of their types and properties. They are considered to be "elementary" particles in the sense that there has been no really successful attempt to treat them as composites of the more familiar elementary particles. Most of the obvious physical characteristics of these particles such as mass, charge and lifetime have been determined. In addition it has proved useful, in classifying these particles and the various reactions which they can undergo, to assign to them certain other intrinsic properties, which can be represented by quantum numbers. The observables corresponding to these quantum numbers are found to be conserved or not conserved in a given interaction depending on the strength of the interaction. For example, although parity is still thought to be conserved in the strong interactions, there are certain types of weak interactions in which it is not conserved.

In particular, the concept of the strangeness quantum number introduced by Gell-Mann[2] and by Nishijima[3] has been remarkably fruitful in classifying and predicting the allowed reactions for strange particle production and decay. Superficially, the interactions between all elementary particles can be divided into three general classes: strong, electromagnetic, and weak; corresponding to time scales of approximately 10^{-23}sec, 10^{-21}sec and 10^{-9}sec respectively. According to the Gell-Mann - Nishijima scheme, the particles which participate in these interactions are assigned various values of strangeness, $S = 0, \pm 1$, or ± 2, and a particle is called strange if it has a non-zero value of S. The total strangeness must be conserved in

the strong and electromagnetic interactions in which the strange particles are produced; whereas its value can change in the weak interactions, through which they decay. This explains the apparently anomalous fact that although the production and decay of the new particles involve only strongly interacting particles, the decay reactions are slower than the production reactions by a factor of 10^{14}. There also have been many other striking confirmations and predictions of this scheme. Although the theory is primarily of a descriptive nature at present, it is hoped that it will lead to a more refined understanding of elementary particles.

In addition to its strangeness, an elementary particle can be assigned various other quantum numbers within the framework of the strangeness scheme. Among these are its electronic charge Q, baryon or heavy particle number M, total isotopic spin T and third component of isotopic spin T_z. These particular quantities are not independent, but are related through the identity $Q = T_z + \frac{M}{2} + \frac{S}{2}$ for each particle. Thus, assuming that charge and the number of heavy particles are always conserved, the conservation or non-conservation of S is equivalent to the conservation or non-conservation of T_z. The whole concept of isotopic spin plays an important role in our present ideas about elementary particles. The hypothesis of charge independence, or conservation of total isotopic spin $\vec{T}$, in the strong interactions has been very successful in so far as reactions involving only pions and nucleons are concerned. Whether or not this useful concept is valid for the strange particle reactions is still a matter for experimental verification.

To put it another way: The assumption that the strong interactions are invariant with respect to rotations about the z axis in isotopic spin space,

i.e., conservation of T_z, has been very successful in describing some of the properties of strange particles such as their long lifetimes and the types of reactions in which they can participate. The more general assumption as to invariance with respect to arbitrary isotopic spin space rotations, i.e., conservation of $\vec{T}$, has yet to be verified. If it turns out to be true, it will be a very useful tool, just as it has been in the case of pions and nucleons. It was hoped that the present experiment would throw some light on this question.

We shall be dealing with two main classes of strange particles: the Σ^+, Σ^o and Σ^- hyperons and the K^+ and K^o mesons. The three Σ's have nearly equal masses ($\sim$1190 Mev) and are assumed to form an isotopic triplet with T = 1 and S = -1. The K^+ and K^o also have nearly the same mass ($\sim$ 494 Mev) and are assumed to form an isotopic doublet with T = 1/2 and S = +1. The reactions

$$\pi^- + p \rightarrow \Sigma^- + K^+ \qquad (1)$$

and

$$\pi^- + p \rightarrow \Sigma^o + K^o \qquad (2)$$

are well established and one would expect, on the basis of strangeness conservation alone, that the reaction

$$\pi^+ + p \rightarrow \Sigma^+ + K^+ \qquad (3)$$

would also occur. This is not a necessary consequence of charge independence, however, since reactions (1) and (2) can take place in a mixed T = 3/2 and T = 1/2 state, whereas reaction (3) is pure T = 3/2. Thus, it is conceivable that the above Σ^- and Σ^o productions would occur (through T = 1/2) while the Σ^+ production would not, because of a possible inhibition of the T = 3/2 production mode. (These effects will be discussed quantitatively in section V).

It was, therefore, of interest first of all to determine whether the reaction (3) could take place, and if so, to what extent could its cross section be reconciled with those of reactions (1) and (2) as regards charge independence. Concerning the first question, there have been several isolated cases of V^+ decays, observed in cloud chambers and emulsions exposed to cosmic rays, which were interpreted as being due to Σ^+ hyperons. In many of these cases the reaction (3) (on nuclear protons) was probably responsible for the production, but in no case was the production process defined so that its identity could be established.

In order to study the proposed reaction, it is desirable to have a well-defined beam of high energy, momentum-analyzed π^+ mesons similar to the beams obtained for π^- mesons at the Cosmotron or Bevatron. In the π^- case they can easily be separated magnetically from the protons which produce them, but a π^+ beam will, in general, have a high proton contamination. Using the external proton beam from the Cosmotron, it became possible to reduce this contamination to a value which would allow a reasonable data-taking efficiency for the University of Michigan twelve-inch propane bubble chamber. The π^+ beam was set up and 22,000 pictures were taken which included 210,000 feet of 1.1 Bev π^+ track.

It was found that the reaction (3) does take place with a total cross section approximately equal to those of reactions (1) and (2). Moreover, this comparison of the total cross sections is certainly consistent with the hypothesis of charge independence. In examining the differential production cross sections for the three reactions, however, the data indicate a disagreement with this hypothesis.

I. EXPERIMENTAL ARRANGEMENT

The π^+ Beam

Early indications of the feasibility of obtaining a relatively pure π^+ beam from the Cosmotron came from some pion-proton total cross section work done by Cool, et al.[4,5]. This led to a further experimental study by Cool, Cronin and De Benedetti to determine the various proton/pion ratios possible, as a function of pion momentum, production angle and target material. This work was carried out with the present bubble chamber experiment in mind and the reader is referred to their paper[6] for a detailed description of the results. The essential features are as follows: The p/π ratio was found to decrease with decreasing atomic number of the target material and with decreasing pion momentum. This particular work was carried out at just one production angle (7^o) but earlier results had indicated that the ratio would also decrease with decreasing production angle. For a desired pion momentum, therefore, one would like to use the lowest Z target and the smallest production angle which are practical. In the course of one of these tests, our bubble chamber was placed in the beam in order to determine what the room background would be like when the Cosmotron intensity was such that an optimum number of particles per pulse passed through the chamber. It was found that the background was negligible, and it was concluded that a bubble chamber experiment to study the reaction $\pi^+ + p \rightarrow \Sigma^+ + K^+$ was entirely possible.

The Beam Set-up

We were led by this study to the experimental beam set-up which is described below. A pion laboratory kinetic energy of 1.1 Bev was chosen in

order to afford a direct comparison of our results with those of a π^- experiment that had already been done at this energy in the same chamber. Figure 1 shows a floor drawing of the arrangement. The 3 Bev external proton beam strikes a 1x1x6-inch polyethylene target at T and produces a spectrum of pions in all directions. The high momentum mesons are produced most abundantly in the forward direction, so the strong focusing magnets H and J were set up to accept a solid angle centering around an angle of 7° with respect to the primary external beam direction. The acceptance angle was limited by the 3x3-inch collimator at (a), and that part of the primary beam which did not interact in the target was dissipated in the lead walls of this collimator and in the iron of the H magnet. The currents in the strong focusing lens were set so as to bring the image of the target to a focus at the one-inch collimator (c). The magnet B deflected the beam through an angle of 23° and provided momentum analysis.

The expected momentum resolution for this set-up can be calculated from the relationship $\frac{\Delta p}{p} = - \frac{\Delta \theta}{\theta}$, where θ is the angle of deflection and $\Delta\theta$ is the differential angle of acceptance. In our case, $\Delta\theta$ is proportional to the sum of the widths of the collimator (c) and that of the target image. From the known properties of the quadrupole lens[7], the target image was calculated to be 0.92 inches wide. This gives an expected resolution of $\pm$ 0.75%. It is desirable to have good resolution because the events are identified mainly on the basis of kinematics. As seen in the diagram, a plastic bag filled with helium was inserted between the magnet B and collimator (c). This was to reduce the broadening of the target image due to

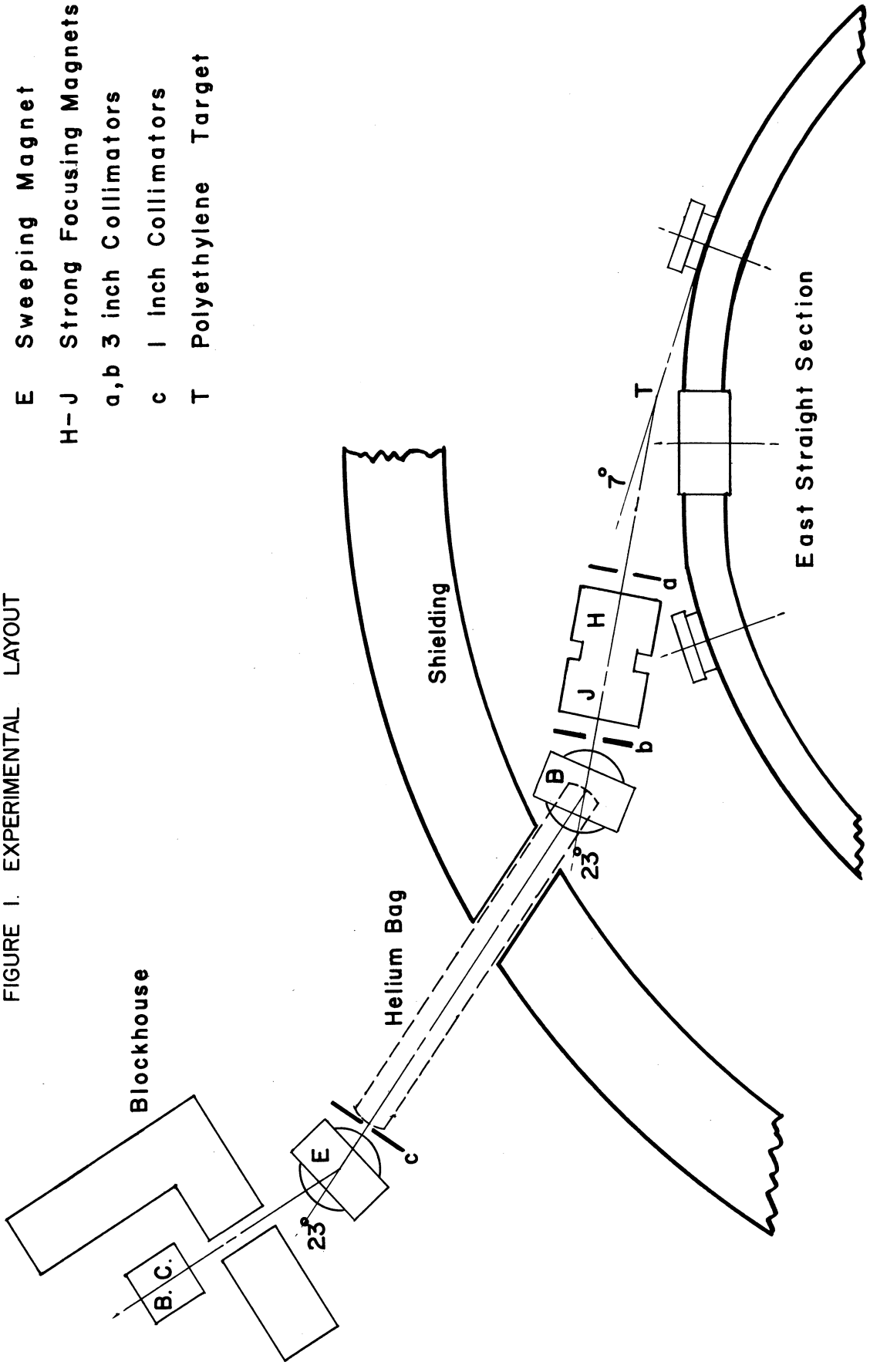

FIGURE I. EXPERIMENTAL LAYOUT

multiple air scattering, which would be appreciable at these distances*[8]. The magnet E did not provide any further momentum analysis, but served mainly to sweep out any low momentum particles which had lost energy in the collimation system. The beam then passed through the bubble chamber (B.C.) which was shielded from the general room background by a concrete block-house. After completing the initial set-up, it was necessary to perform a wire measurement on the system to insure proper alignment. A wire was suspended between the target and the chamber, and the current and tension adjusted so as to correspond to the desired momentum 1.232 Bev/c. Fine adjustments were then made so that the wire passed through the center of the collimators.

An important factor in the success of the experiment was the use of the rapid beam ejector developed at Brookhaven by D. C. Rahm[9]. This device reduces the duration of the beam pulses to a few microseconds, as opposed to a minimum of about two milliseconds without it. Due to the rapid bubble growth in propane, a two millisecond pulse will produce tracks which differ greatly in bubble size, whereas with the rapid beam ejector in operation they can be made uniformly small. This not only reduces measurement error but, in our case, allowed us to have almost twice as many tracks per picture without affecting their ability to be scanned easily.

Counter Measurements

Beam Width

The sensitive volume of the bubble chamber is 5x5x12-inches with the beam entering through the 5x5-inch cross section. Thus, it was desirable

* The r.m.s. deviation of a particle of our momentum passing through 30 feet of air would be about 1 cm. Helium reduces this by a factor of 30.

to have a beam which was somewhat narrower than five inches upon entering the chamber. This reduces the chances of losing sight of an interaction which occurs near the front or back window of the chamber and also reduces the background of stray particles which come from interactions in the glass or aluminum walls. The width of the beam at the chamber is determined by its angular divergence after passing through the focus at (c) and the additional spreading of the momentum components due to the sweeping magnet E. The collimation system was arranged so that an extreme-ray calculation gave a beam width of four inches for a beam with a momentum spread of $\pm$ 0.75%. Its height was also restricted to three inches by the three-inch-high collimators.

In order to check the beam width, a counter was moved laterally across the entrance side of the chamber and a plot made of intensity vs. position. The curve showed a maximum at about 1/2-inch from the center of the chamber, and 95% of the beam fell within an interval of two inches on either side of this maximum. This agrees well with the 100% width of four inches that was calculated from the geometrical set-up and expected momentum spread, and confirms the fact that the momentum resolution was $\pm$ 0.75%. However, variations which were observed in the analyzing magnet field must be independently added to this to give a final beam momentum of P = 1.232 Bev/c $\pm$ 1.5%. The expected width and height of the beam were also confirmed later by observation of the actual distribution of tracks in the pictures.

Proton to Pion Ratio

In order to calculate the cross sections for any observed processes, it is necessary to know the ratio of protons to pions which pass through the chamber. Actually the beam contains not only p and π^+, but also a small

contamination of μ^+ which must be taken into account. The pions and muons have practically the same velocity ($\beta = 0.99$), whereas the protons are significantly slower ($\beta = 0.79$) and can be separated electronically from the higher velocity component of the beam. A time-of-flight technique was used, similar to that of Cool, Piccioni and Clark.[10].

A counter telescope was placed in the beam with one pair of counters just outside the Cosmotron shielding and the other pair immediately in front of the bubble chamber. The distance between the counters was 20 feet, which corresponds to a difference of 5.2×10^{-9} seconds between the flight times of the protons and mesons. The amount of delay necessary to bring the two pairs of counters into coincidence measures the flight time of the particles. Curves were plotted of intensity vs. delay time for both positive and negative beams of momentum 1.232 Bev/c. The intensity was normalized with a monitor counter and is plotted against the delay in feet of RG-63, as shown in Figure 2. The zero point of the abscissa was arbitrarily chosen to be at the center of the negative beam curve. Since the negative beam consists of pions and muons only, it gives the delay curve for a pure beam of $\beta = 0.99$ particles. Curve II is the one obtained for the positive beam and clearly shows the two velocity components. Since the width of the curves is due only to the pulse widths from the counters, it is the same for all velocity components, and the leading edge of curve II can be assumed to be due solely to the high velocity component of the positive beam. Thus, the negative beam, Curve I, is normalized to follow this leading edge, and the difference between II and I gives the proton delay Curve III. This has the same shape as Curve I, and is shifted by an amount corresponding to the predicted difference in flight time. The relative heights of Curves III and I, then, give the ratio of protons to pions and muons. This

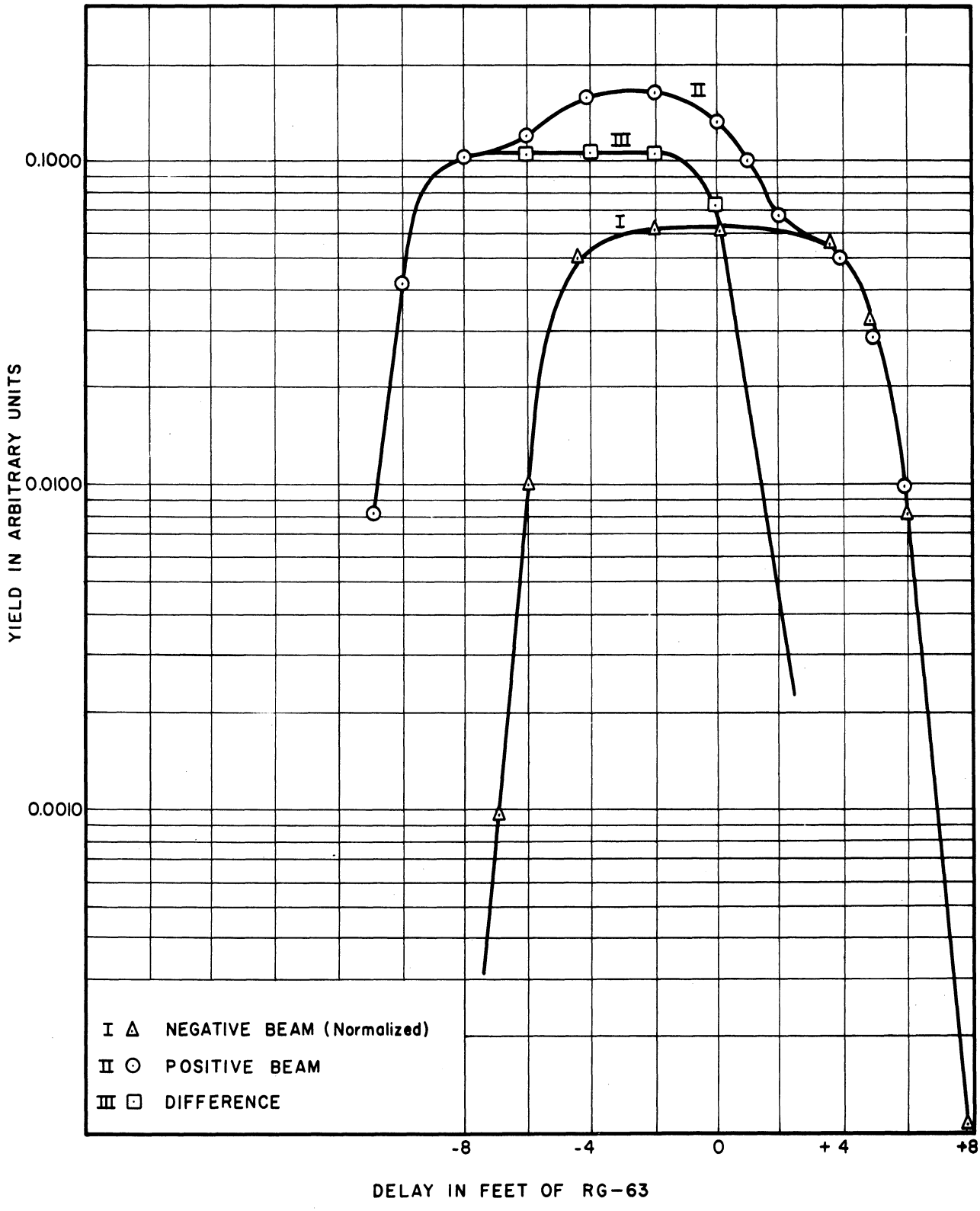

FIGURE 2 DELAY CURVES

ratio is 1.75 $\pm$ 0.09. The errors quoted are due partly to statistics and partly to an uncertainty in normalizing Curve I to the leading edge of Curve II.

By previous measurements in similar beams[10], it was estimated that the muons represent a contamination of (8 $\pm$ 3)% of the pions.

II. THE BUBBLE CHAMBER

Figure 3 is a line drawing of the bubble chamber and associated equipment. The chamber itself is made of aluminum, and has a sensitive volume of 12x5x5-inches. It was operated at 51.9°C with a pre-expansion pressure of 375-400 psi. The vapor pressure of the propane at this temperature is 250 psi. The temperature was controlled by means of thermistor circuits. Expansion and recompression were carried out by air pressure applied to a rubber diaphragm in contact with the propane. The diaphragm was made of a piece of 1/8" butyl rubber sandwiched between two pieces of 1/32" teflon. A 3/4-inch, three-way Barksdale valve actuated a larger poppet valve to provide expansion.

A line source of light was provided for the bright-field photographic scheme by means of two xenon-filled flash tubes. The flash duration was about 40 microseconds, and intense enough to allow the camera lenses to be stopped down to f45. This provided a depth of field sufficient to have all parts of the chamber in good focus. Separate strips of 70mm film were used for the two stereo photographs. The film was held flat by means of pressure plates and vacuum backs in the camera.

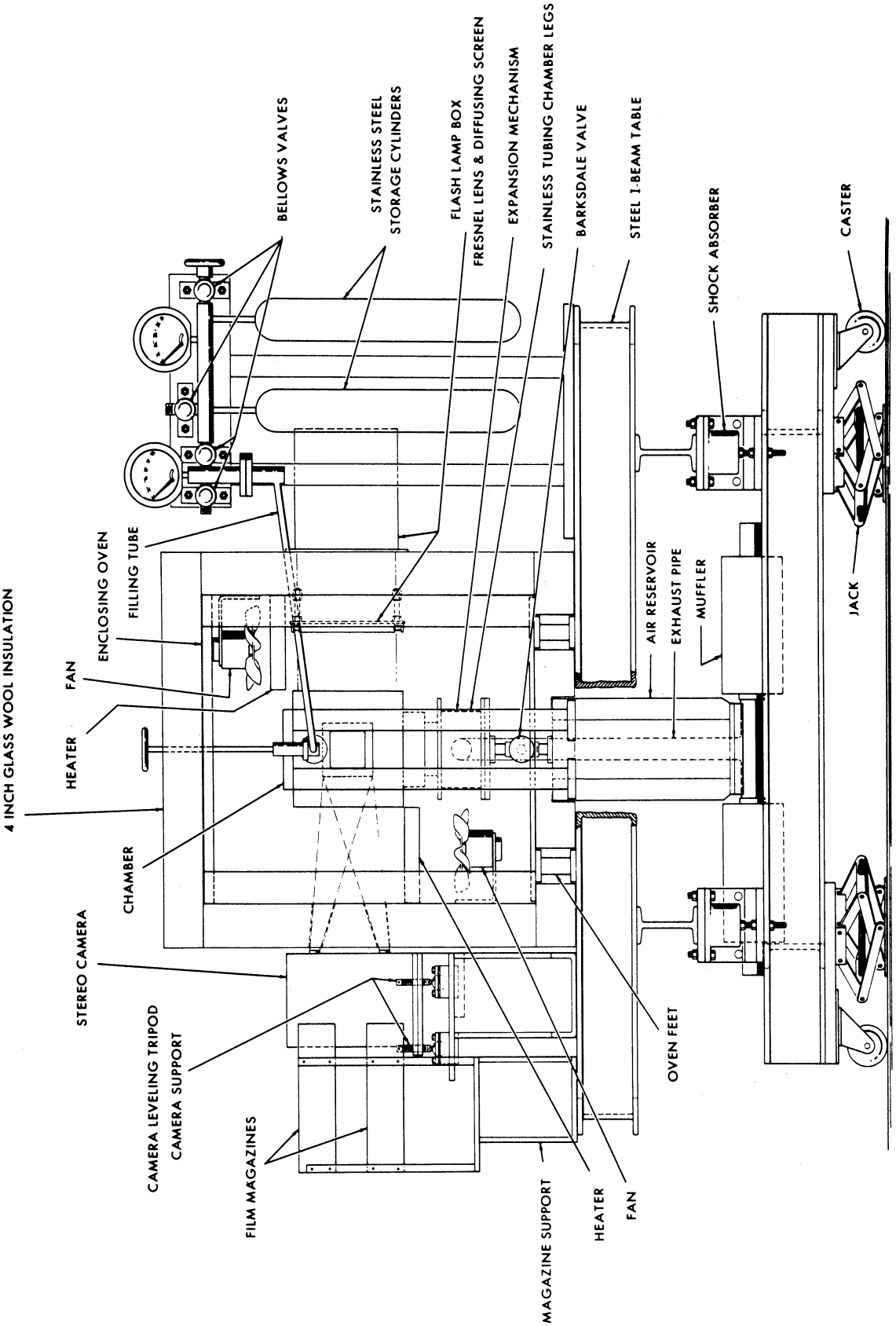

FIGURE 3. 12 INCH BUBBLE CHAMBER WITH STEREO CAMERA, OVEN, PLUMBING, AND SUPPORTING STRUCTURES.

III. REDUCTION OF DATA

Scanning

Some of the properties of the Σ^+ are well known from the reaction

$$K^- + p \rightarrow \Sigma^+ + \pi^- ,$$

which has been studied by various emulsion workers and in the University of California hydrogen bubble chamber. It was found that the Σ^+ could decay via two modes with about equal probability:

$$\Sigma^+ \rightarrow \pi^+ + n$$

or

$$\Sigma^+ \rightarrow \pi^\circ + p$$

In our case, the reaction

$$\pi^+ + p \rightarrow \Sigma^+ + K^+$$

will appear as a Y-shaped event, the proton being at rest in the propane (C_3H_8). In order to be recognized by the scanners at least one of the arms of the Y must show a kink (i.e., possible decay) somewhere along its path. At our energy, the relativistic kinematics of the reaction restrict the Σ^+ to a maximum angle of about 25°, and the K^+ to a maximum angle of about 65° with respect to the line of flight of the incident π^+. The sum of the two angles must always be less than 70°. Since the incident pion tracks are parallel to the film plane and the events must be coplanar, these real angles, when projected on the film, can appear smaller but not larger. Thus, the scanners were instructed to area-scan for kinked Y's with the following properties:

1. At least one of the arms of the Y must come off at an angle less than 25°.

2. The other arm must be less than 65°.
3. The included angle must be less than 70°.
4. The extension of the π^+ line of flight (trunk of the Y) must lie between the two arms of the Y.
5. There can be no extraneous prongs coming off either at the origin (which would indicate a carbon event) or at the kink (which would indicate a scattering instead of a decay).

Events which passed this rough scanning were found at the rate of about one every thirty pictures. These were then fine-scanned and about two-thirds of them rejected on the basis of sharper angular restrictions, bubble densities, and particles which were identified by stopping in the chamber. Events which passed the fine scanning were then measured.

Measurement and Computation

Co-ordinates of points on the film were measured directly on the two stereo negatives by means of a traveling microscope arrangement, which reads to the nearest 1/1000 of an inch. The typical bubble diameter was about .004 inches (on the film), and all points to be measured were formed either by the intersection of two tracks, or could be chosen arbitrarily along a track. Thus, there was, in general, no difficulty in setting the microscope with the above precision. The film co-ordinates were then punched on cards and the co-ordinates of points and the angles in the bubble chamber were calculated with the aid of the University's I.B.M. 650 computer. The constants in the conversion formulae were evaluated by means of a series of fiducial marks of one centimeter spacing on the front and back windows of the chamber.

Accuracy

A direct indication of the accuracy with which the computed angles approximate their true values can be obtained by measuring a number of events for which the true angles are known. For this purpose, we have considered the results of such measurements on forty elastic p - p scatterings. The kinematics of the reaction $p + p \rightarrow p + p$ define a unique relationship between the angles θ_1 and θ_2 of the outgoing protons, which is represented by a curve on θ_1 vs. θ_2 plot. The curve and the distribution of the forty scatterings along it, are shown in Figure 5. The background is low so that at most probably two or three of these events are not true p - p scatterings. The deviations ($\Delta\theta$) of the measured angles from this curve are plotted in the first histogram in Figure 4 which shows that the angular inaccuracy for events of this type would be represented by a circle of about one degree radius.

Since the scattering events are two-body processes with one of the protons initially at rest, they must also satisfy the requirement that the incoming and two outgoing tracks be coplanar. The second graph gives the measured angles of non-coplanarity Φ_c for these forty scatterings. From these two graphs one would tend to reject any event which showed a deviation of more than one degree from a given kinematic curve or had a non-coplanarity angle of greater than one degree. However, for events in which the length of the shortest track is less than one centimeter, or which are obscured in the chamber for some reason, we cannot expect to obtain this accuracy. The inherent inaccuracy for any particular event of this type can always be determined by several re-measurings.

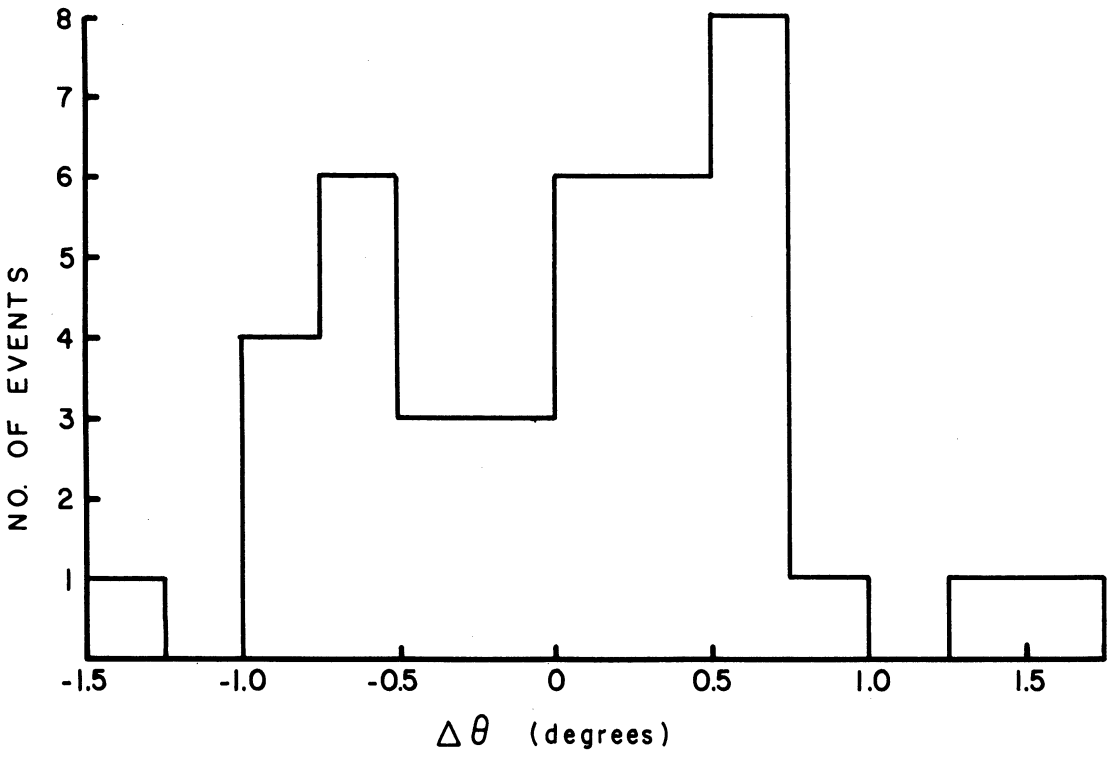

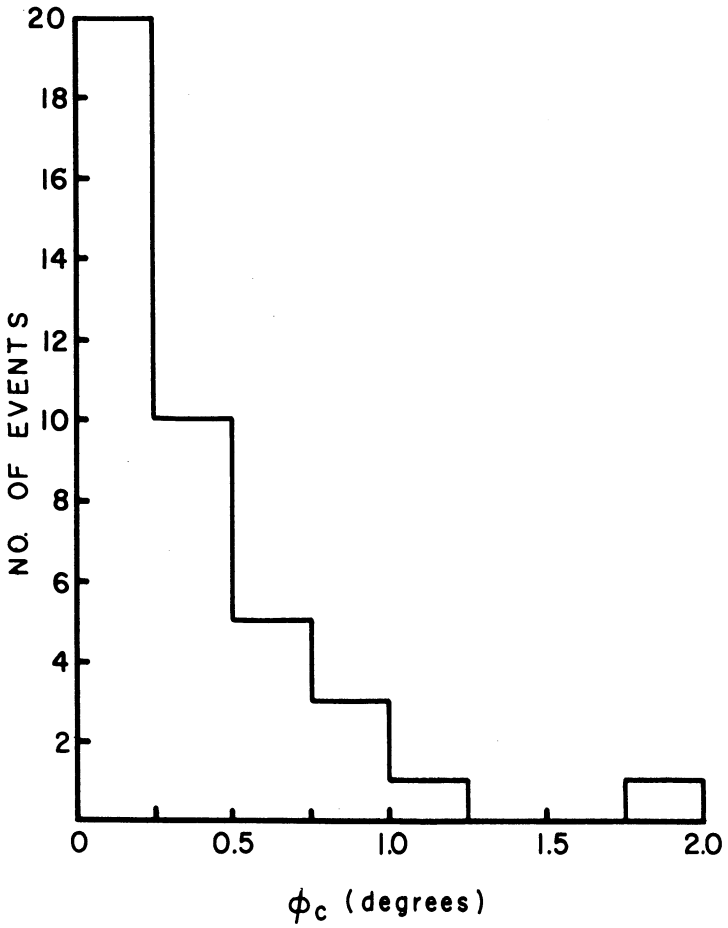

FIGURE 4 MEASUREMENT ACCURACY HISTOGRAMS

IV. IDENTIFICATION OF EVENTS

The kinematic restrictions on any reaction of the type a + b $\rightarrow$ c + d (where b is at rest) can be represented by a curve on a θ_c vs. θ_d plot. θ_c and θ_d are the laboratory angles of the outgoing particles with respect to the incident direction of particle a. These curves are based on the requirement of the conservation of relativistic energy and momentum, and their form is determined by the masses of the four particles and the kinetic energy of particle a. In Figure 5, is shown the curve for the reactions $\pi^+ + p \rightarrow \Sigma^+ + K^+$, and a portion of the curve for $p + p \rightarrow p + p$. The struck proton represents one of the hydrogen atoms in the propane, and therefore, can be considered to be at rest. The double $\Sigma^+ - K^+$ curve indicates the incident momentum spread of $\pm$ 1.5%. The numbers on the lines connecting the two curves denote the production angle of the Σ^+ in the center of mass of the π - p system. In the p - p case, this momentum spread turns out to be much smaller than the measurement inaccuracy and, therefore, is not shown. The π - p elastic scattering curve lies above the p - p curve and is not plotted.

If there were nothing but free protons in the chamber, the identification of $\Sigma^+ - K^+$ events would be extremely simple. The presence of the carbon atoms, however, complicates the situation considerably. The points on the graph represent all of the kinked Y's which passed the scanning criteria and whose measured angles of non-coplanarity were less than 1.5°. Most of the non-identified events are double scatterings in carbon in which the second scattering produced no visible prongs and, therefore, looked like a possible decay to the scanners. This large background indicates that coplanarity is by no means a sufficient test to insure that a given event is a two-body hydrogen process. The identification of $\Sigma^+ - K^+$ productions must be based

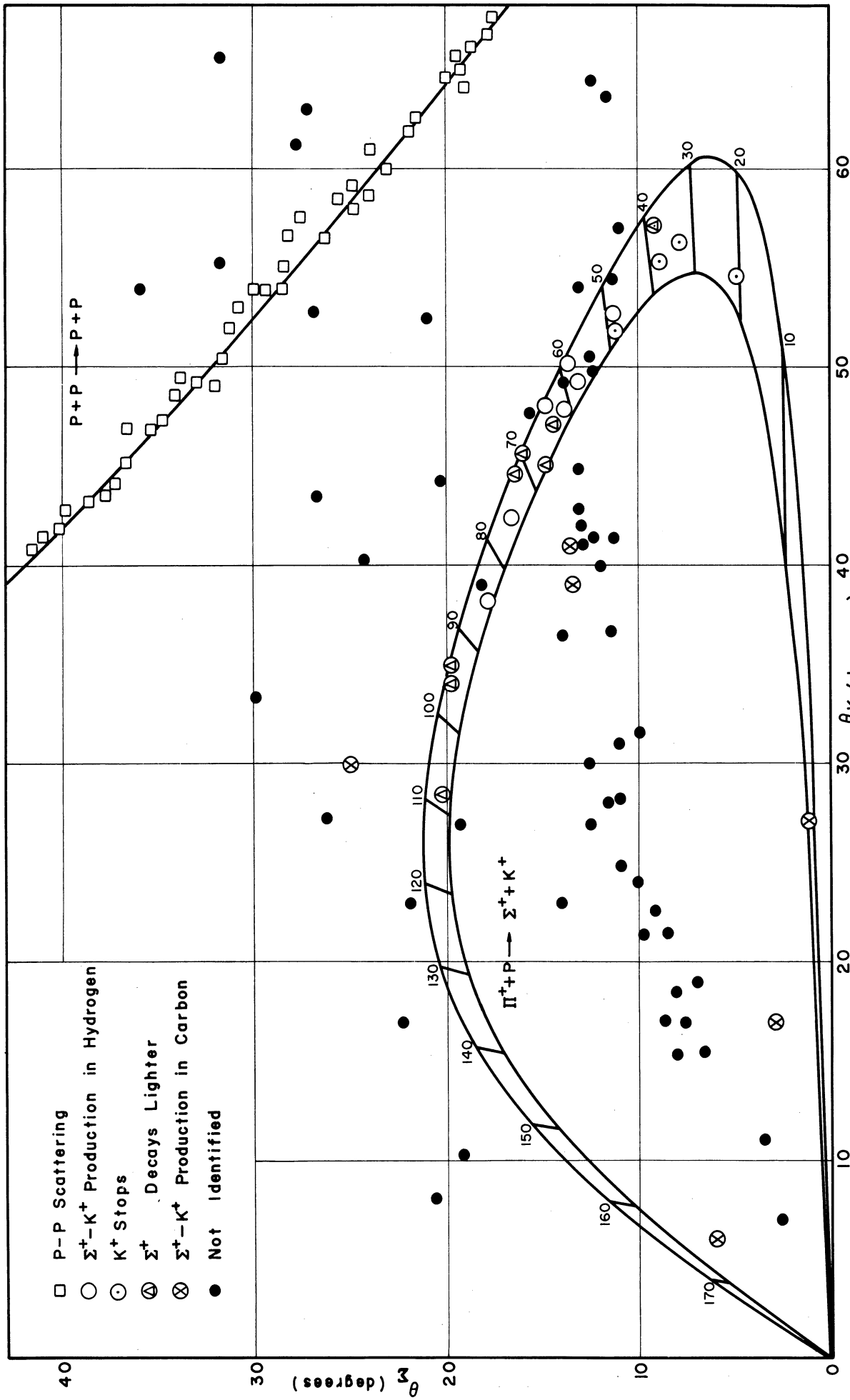

FIGURE 5 KINEMATIC PLOT

mainly on the angular restrictions. In addition to this, however, these Σ^+ - K^+ events will often show particular characteristics which aid in their identification. A K^+ which stops and decays in the chamber can easily be recognized, and the additional information obtained by measuring its range provides a further check on the reaction. Another signature comes from observing a change in bubble density between the parent and daughter tracks at the decay of the Σ^+. The bubble density of a particle varies inversely as the square of its velocity[11], and from the production and decay kinematics of the Σ^+ the velocities of the particles involved can be calculated. Assuming that the Σ^+ decays isotropically in its center-of-mass frame, we can estimate that its decay should show a decrease in bubble density about 90% of the time for the π^+ decay mode, and about 50% of the time for the proton decay mode. In some of the cases, this decrease can be recognized easily by inspection; in others it can be detected by actual bubble counting. In some cases, however, in which the predicted velocity of the daughter particle is not significantly greater than that of the parent, the effect is too slight to be confirmed. When it <u>can</u> be confirmed, it indicates that the observed kink was a true decay and not simply a prongless carbon scattering. The events which showed these characteristics of stopping K's or Σ^+ decays into a lighter track are designated on the curve in Figure 5.

Using these events, for which the identification as being Σ^+ - K^+ hydrogen productions was quite certain, it was possible to calibrate the kinematic curve with respect to the expected bubble densities of the Σ^+ and K^+ particles themselves in a hydrogen production. The criterion of bubble density was used in a qualitative way only; classifying tracks as heavy, medium heavy, medium, medium light, or light; with respect to the incident (minimum ionizing)

pion track. It was essential always to determine bubble density relative to the minimum tracks on each picture as the bubble density for a particle of given velocity can vary from picture to picture. The calibration of the curve with respect to bubble density showed the following features: Proceeding around the curve in the counterclockwise direction, the K^+ bubble density varies from heavy (just before stopping) to medium light near the 100° line; on the other hand, the Σ^+ bubble density varies from light to medium heavy over this same range. The fact that the bubble density of the particles was such a sensitive function of their position on the curve was very useful in rejecting spurious events which happened to fall between the kinematic curves. Thus, in order to be classified as $\Sigma^+ - K^+$ production, the event had to satisfy the following requirements:

1. The laboratory production angles of the Σ^+ and the K^+ must be consistent with the kinematics (including coplanarity) of the reaction $\pi^+ + p(\text{at rest}) \rightarrow \Sigma^+ + K^+$ within the allowed beam momentum spread.
2. The ranges and bubble densities of the Σ^+ and K^+ must agree with their calculated momenta.
3. The decay process of the Σ^+ must also satisfy these requirements of kinematics, range and bubble density.

The nineteen events which satisfied these criteria are shown in Figure 5. Whenever an event fell near the curve and had the correct bubble density, it was remeasured until its production angles became well-defined. For each individual case, a correction was made for the average energy loss of the incident pion before the production occurred. This was of the order of one or two percent of the incident momentum, depending on how much propane

and aluminum the pion traversed. In all nineteen cases the Σ^+ decayed in the chamber and in one case the K^+ decayed in flight. There were five instances in which the K^+ came to rest and decayed in the chamber, one of which is shown in Figure 6. The additional information obtained in this way from the K^+ range, allowed a check on the beam momentum. The percentage variations from the expected mean momentum of 1.232 Bev/c for these five cases are shown in Table I.

TABLE I. BEAM MOMENTUM FROM STOPPING K^+

Event No.	Calculated ΔP_{inc} (%)
68696	-0.6 ± 0.3
69905	-1.0 ± 0.2
74866	-0.5 ± 0.5
81602	-0.2 ± 0.6
86759	$+0.3 \pm 0.2$

These all fall within the momentum spread of $\pm$ 1.5% and their mean value is -.4%, indicating a true mean momentum of 1.227 Bev/c. The fact that the mean is not 1.232 Bev/c is not surprising because of the inaccuracies involved in making the wire measurement during the beam set-up. The curves in Figure 5 were, therefore, plotted for a beam momentum of 1.227 Bev/c $\pm$ 1.5%.

Another way to understand the basis on which the identification of $\Sigma^+ - K^+$ productions is made, is as follows. In the reaction $\pi^+ + p(\text{at rest}) \rightarrow \Sigma^+ + K^+$ there are five unknowns (assuming that all masses are known) involved in the kinematical equations. These are the magnitudes of the momenta of

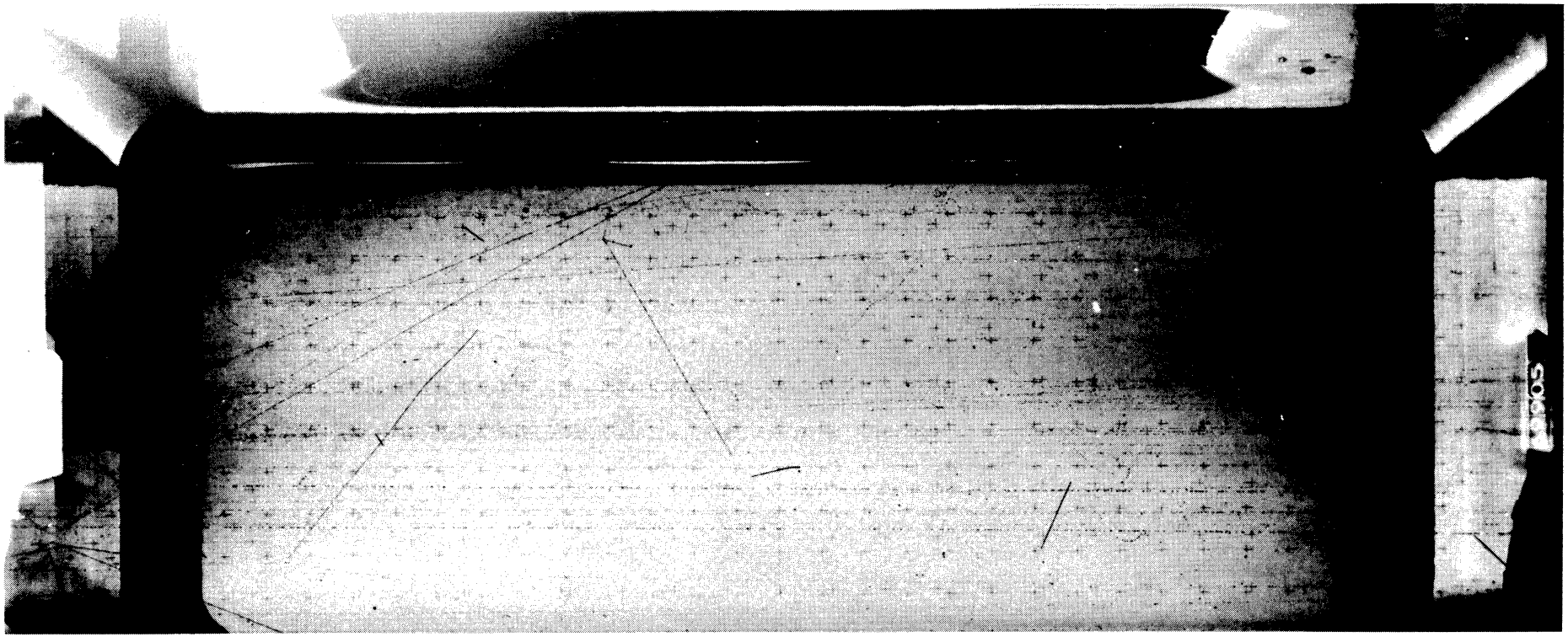

FIGURE 6. AN EXAMPLE OF THE REACTION $\pi^+ + p \rightarrow \Sigma^+ + K^+$

The π^+ enters in the lower left hand corner and produces the reaction after moving a few centimeters in the chamber. The K^+ proceeds upward and to the right, and after traveling about six centimeters stops and decays into a lighter particle. The Σ^+ goes downward to the right and after about two centimeters decays into a π^+ and a neutron (not visible).

the π^+, Σ^+ and K^+; and the production angles of the Σ^+ and K^+ with respect to the pion direction. Relating these five unknowns, there are three equations, two from the conservation of linear momentum and one from the conservation of energy. Thus, by measuring any two quantities the other three can be calculated. In general, Σ^+ - K^+ events are identified by measuring the two production angles and then calculating the π^+ momentum to see if it agrees with the expected value. From this point of view, the events listed in Table I, in which the K^+ momentum was also measured, are kinematically overdetermined, and there can be little doubt that they are examples of the above reaction. The values of ΔP_{inc} in Table I were calculated using the K^+ range and its production angle, the errors being due mainly to errors in measuring the angle. Since the beam momentum is not a very sensitive function of the K^+ range, this gives a more accurate determination of P_{inc} than would be obtained by using the two measured production angles.

Of the remaining fourteen events which satisfied the kinematics and bubble density requirements, seven were distinguished by the fact that the Σ^+ decayed into a lighter track, and in one case the K^+ decayed in flight into a lighter track. The identification of these lighter-decay events is also fairly certain, as the possibility that they are double scatterings can be ruled out.

The final six events were classified as Σ^+ - K^+ productions on the basis of kinematics and bubble density alone. They have two additional arguments in their favor, however: There are five other events which fall between the kinematic curves but do not have the correct bubble density. This is just about the number one would expect by projecting the general background of events outside the curves into the region between the curves.

If we did not call these last six events Σ - K's, this would bring the background up to eleven which is clearly too high. The second argument is based on the bubble density of the Σ^+ decay product. About three-fourths of the π^+ decays, and one-third of the proton decays should be detectably lighter. This is not considering the events in which the K^+ stops, for which the Σ^+ track is already classified as "light." Thus, there should be at least a few events where the K^+ does not stop, which show a non-lighter decay. These qualifications are satisfied by the six events in question, four of which were classified as decays into protons.

Having distinguished between Σ^+ - K^+ productions and double scatterings in the manner described above, we still must consider Σ^+ - K^+ productions which occur on protons in the carbon nuclei. There are eight free protons and eighteen carbon protons in each propane molecule, and thus, we might expect about twice as many carbon events as hydrogen events. The fact that the carbon nucleons are closely bound and, therefore, shade one another probably reduces their effectiveness. Results from other experiments indicate that the ratio of carbon to hydrogen events is actually about 1.5. A more thorough study of these effects is being made.

Since the carbon protons have a binding energy and Fermi momentum within the nucleus, these carbon Σ - K's will, in general, not be truly coplanar. However, as we have seen, coplanarity is not a very good test and we can expect an appreciable fraction of the carbon productions to satisfy our coplanarity requirements. These apparently coplanar events can be explained as follows: The de Broglie wave length of the beam particles is 1.0×10^{-13}cm which is smaller than the proton radius and, thus, interactions with individual nucleons can be expected. The binding energy of the protons is negligible at these

energies, and there will be little momentum transfer to the nucleus, provided the particles do not suffer any secondary collisions before getting out. If secondary collisions do take place, there is a good chance that the event will be measurably non-coplanar and also have extraneous prongs associated with it. As concerns the possible confusion of these carbon events with hydrogen events, we are only concerned with the prongless, "coplanar" cases. These probably occur most frequently on peripheral protons where the chances of secondary collisions are small.

Six of these prongless coplanar carbon events were found and are shown in Figure 5. One of these was identified by a stopping K, and the other five by lighter decays. There was an additional event found by the scanners in which the K^+ stopped, which was prongless, but non-coplanar. There were undoubtedly other carbon productions present which were not recognized, either because they showed no particular decay characteristics or because their angles on the film were such that they were rejected by the scanners. Some of these are probably among the "non-identified" events in Figure 5.

To assure ourselves that an appreciable number of what we call "hydrogen productions" were not actually carbon productions which happened to be prongless and coplanar, a study was made of the expected distribution of carbon $\Sigma^+ - K^+$ events on the θ_Σ vs. θ_K plot. This study was based on the following assumptions:

1. For the prongless coplanar events under consideration, which presumably do not suffer secondary collisions, the kinematics for the reaction $\pi^+ + p \rightarrow \Sigma^+ + K^+$ can be calculated assuming that the proton is unbound but possesses a Fermi momentum. The binding energy of the proton is neglected.

2. The total production cross section is constant for the various center-of-mass energies considered.

3. The differential production cross section is the same for carbon protons as for free protons.

The distribution of Fermi momentum was taken to be a three-dimensional Gaussian of the form $p^2 \exp(-p^2/p_o^2)\, dp$, which is proportional to the probability of finding a proton with total momentum in the interval $(p, p + dp)$. This curve has a broad maximum around p_o which was taken as 190 Mev/c[12]. It turns out that the position and shape of the kinematic curves is a very sensitive function of proton momentum components in the forward and backward directions with respect to the line of flight of the incident pion. For example, giving the proton only 40 Mev/c in the forward and backward direction will produce two curves, one of which falls well inside and the other well outside the momentum limits on the hydrogen curve in Figure 5. This marked sensitivity is due not so much to the change in the total energy of the system as to the change in the velocity of the center of mass. This change in velocity has a large effect on the relationship between the center-of-mass angles and the laboratory angles and, thus, produces the wide separation of the curves. In other words, two identical center-of-mass angles can correspond to widely different laboratory angles if the center-of-mass velocity for the two cases is not the same. For forward and backward protons, the interpretation of the carbon kinematic curves is simple and unambiguous, but in cases where the proton has a momentum component perpendicular to the pion direction, the situation is more complicated. Since the azimuthal angle of the proton momentum vector with respect to the pion momentum vector is not defined, the computed angles, Θ_Σ and Θ_K, must be referred to the total momentum vector of

the system. However, the measured angles, Θ_Σ and Θ_K, are always taken with respect to the π^+ line of flight. Thus, a given carbon event cannot be represented by a point $(\Theta_\Sigma, \Theta_K)$ on the kinematic plot, but must be represented by a curve connecting the two points $(\Theta_\Sigma + \alpha, \Theta_K - \alpha)$ and $(\Theta_\Sigma - \alpha, \Theta_K + \alpha)$; where α is the angle between the total momentum and the pion momentum. These curves are not straight lines of slope -1 connecting the two end points, but are slightly convex upward, depending on the size of Θ_Σ, Θ_K and α. The two end points correspond to truly coplanar carbon events and the intermediate points represent the other possible values of the measured Σ^+ and K^+ angles. These intermediate points will always be non-coplanar (but may be not measurably so), the maximum angle of non-coplanarity being α.

For purposes of estimating the possible carbon contamination, 250 carbon events were mocked-up as follows: Five proton momenta were chosen at intervals representing equal areas under the three-dimensional Gaussian curve. For each of these momenta, five angles of the proton momentum with respect to the pion momentum were chosen at equal intervals of the cosine. For each of these twenty-five cases, ten values of the Σ^+ center-of-mass production angle were chosen, representing equal intervals of area under the Σ^+ hydrogen center-of-mass production curve, shown in Figure 7, on the following page. The various angles Θ_Σ and Θ_K for these 250 events were then computed with the I.B.M. 650. By examining the curve connecting the two points $(\Theta_\Sigma + \alpha, \Theta_K - \alpha)$ and $(\Theta_\Sigma - \alpha, \Theta_K + \alpha)$ for each event, an estimate was made of the probability that the event would satisfy the hydrogen production kinematics. Only portions of the curve for which the computed non-coplanarity angle was less than three degrees were considered. Range and bubble density criteria were also used whenever they were definite. Out of these 250 mock events, only 2.4

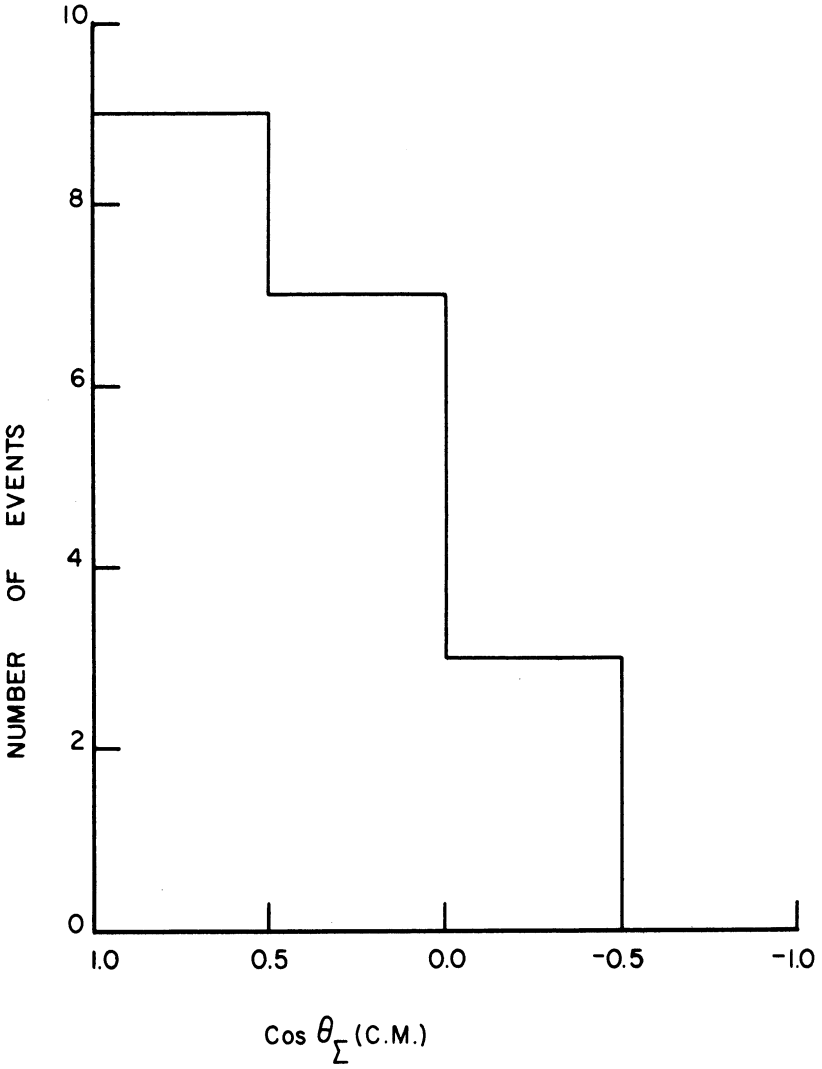

Σ^+ CENTER OF MASS PRODUCTION ANGULAR DISTRIBUTION

FIGURE 7

events satisfied the hydrogen acceptance criteria, indicating a probability of only about 1% for a random carbon Σ^+ - K^+ production to be confused with a hydrogen production.

Thus, there is little chance that even one of our Σ^+ - K^+ events is due to carbon. The greatest source of error in identification would come from

the possibility of mistaking a double scattering for a hydrogen production. It is also possible that we have underestimated the number of hydrogen events since there were two events which fell in the region of the hydrogen curve, but were obscured in the chamber so that their measurement and bubble density determination were too difficult to allow positive identification.

Thus, on the basis of identification uncertainty alone, we would say that the number of hydrogen $\Sigma^+ - K^+$ productions found was 19 ± 2.

V. PRODUCTION PROCESS

Total Cross Section

The following factors were taken into consideration in calculating the total cross section.

1. Total number of tracks: The total number of tracks scanned was estimated by having the scanners count the incoming beam tracks on every fiftieth picture. The mean number of tracks per picture from this sample was 28.8 and, because of the size of the sample, the error in determining the mean of the total population in this way was only about $\pm$ 2%. Of the 22,000 pictures taken, about 1,000 were lost either in the developing process or because they were unscannable. Thus, the total number of tracks scanned was $(28.8 \pm .63) \times 21{,}000 = 604{,}000 \pm 13{,}000$. This includes protons, pions and muons.

2. Proton to pion ratio in the beam: In section II, the measured ratio of heavy particles to light particles in the beam was found to be $p/(\pi + \mu) = 1.75 \pm .09$, and it was estimated that $\mu/(\pi + \mu) = .08 + .03$. Thus, the fraction of all the beam tracks which were due to positive pions is $\pi/(p + \pi + \mu) = .334 \pm .015$.

3. Beam attenuation: Due to the total interaction cross section for pions of this energy in propane, an appreciable fraction of the beam is lost before reaching the end of the chamber. This amounts to a 10% correction in the total number of tracks scanned.

4. Density of the propane: The density of the propane under operating conditions was determined by measuring the lengths of muon tracks in the $\pi - \mu - e$ decay. The resulting density was 0.45 gm/cm^3 which is in good agreement with the value estimated thermodynamically. This work was performed by T. Zipf.

5. Number of events: The number of events found in the first scanning was 18. Due to the uncertainty in identification and the statistical fluctuation, this number is taken to be 18 ± 5. This is the source of the largest error in the estimation of the cross section.

6. End effects: The average Σ^+ path length was 2.5 cm, and therefore, events which occured near the end of the chamber might easily have been missed due to the Σ^+ decaying outside. Taking this into account and allowing an additional 1/2 cm needed for identification at the entrance end of the chamber, the correction in the cross section due to these end effects is taken as 10%. A similar effect due to the sides of the chamber is negligible, since the beam was confined to the central portion of the chamber and the sigmas are produced at angles of less than 25°.

7. Short decays: As will be seen in section VI, there was a certain cut-off in the Σ^+ path length below which the scanning efficiency was very low. Undoubtedly there were events missed because the Σ^+ decayed very close to the origin. Taking this cut-off length as 0.4 cm (see Figure 8) we can estimate that the fraction of events missed in this way was $1 - \exp(-0.4/2.5) = 0.15$. The validity of this number was checked by examining the differential lifetime decay curve for the observed sigmas, where it was seen that three of four decays were clearly missing at the short end.

8. Scanning efficiencies: Of the eighteen observed Σ^+'s, fourteen decayed via the mode $\Sigma^+ \rightarrow \pi^+ + n$, and four via the mode $\Sigma^+ \rightarrow \pi^\circ + p$. Due to the high Σ^+ momentum (about one Bev/c) the proton in the latter case is restricted to laboratory angles of less than about 15° with respect to the Σ^+ line of flight. In the first mode, the π^+ is unrestricted as to angle.

Thirteen of the fourteen π^+ decays were, therefore, positively identified because their decay angles were too large to be protons. The remaining five cases were differentiated on the basis of bubble density. The ratio of proton decays to π^+ decays of 4/14 is quite small when compared with that obtained in the K^- absorption experiments in the hydrogen bubble chamber and in emulsions. Combining the data from all these experiments, one finds a branching ratio of about 0.9. The low value obtained in our experiment can be explained as being due to a scanning bias against the small angle proton decay, as will be seen below. On the other hand, the Σ^+ produced in a K^- absorption reaction is relatively slow, its moderation time being comparable to its mean life, so that there is no bias due to angle in this case. There is, in fact, probably a small bias <u>against</u> the π^+ mode in the emulsion observations due to its lighter ionization as compared with the proton.

In order to determine scanning efficiencies, a careful rescanning was made of 4,000 pictures. Because of the larger numbers available, all events which satisfied the rough scanning criteria were used in determining efficiencies. The events found in the rescanning were divided into two classes: "π^+ type," in which the decay angle was greater than 15° (on the film) and "proton type," in which the decay angle was less than 15°. The proton type events were further subdivided into two classes, one with decay angles of less then 5° and one with decay angles between 5° and 15°. Upon averaging over center-of-mass decay angle and dip angle in the chamber, it was estimated that 40% of the real $\Sigma^+ \rightarrow \pi^\circ + p$ decays should fall in the first category and 60% in the second category, assuming that the decay process is isotropic in the center-of-mass. It was found that for decay angles

of less than 5° the scanning efficiency was 0.25 ± 0.10; for angles between 5° and 15° it was 0.60 ± 0.10; and for angles greater than 15° it was 0.75 ± 0.10. The average detection efficiency for proton-type events was, thus, only 0.60 x 0.60 + 0.40 x 0.25 = 0.46, whereas for the π^+ type, it was 0.75. It is felt that this bias against the proton decay mode is the most reasonable explanation for the low observed branching ratio. There was one additional real $\Sigma^+ - K^+$ production found in the rescanning which was identified as a proton-type decay.

Taking all of the above factors into account, one finds for the total cross section for the process $\pi^+ + p \rightarrow \Sigma^+ + K^+$,

$$\sigma(+) = 0.15 \pm 0.05 \text{ mb.}$$

Any systematic errors which have escaped our attention would probably tend to increase this number.

Differential Cross Section

The production angular distribution for the nineteen observed events is shown in Figure 7. The abscissa is the cosine of the Σ^+ center-of-mass production angle. The distribution is strongly peaked forward and indicates that there must be at least p-waves taking part in the production process. It is not felt that there can be any scanning bias against the larger production angles. Although the large angle sigmas would be moving slower and, therefore, have a somewhat greater loss due to short decays, this effect is actually negligible since the Σ^+ momentum varies only by a factor of two around the kinematic curve (Figure 5). Using the scanning efficiency cut-off length $l_0 = 0.4$ cm (Figure 8), this means that the slowest possible Σ^+ would have a detection probability of 0.9 of that of the fastest possible Σ^+. This small effect should be more than compensated for by the

fact that the proton decay angle can be as large as 30° for the slower sigmas so that actually there is probably a slight bias in favor of the hyperons produced at large angles.

In comparing the above $\Sigma^+ - K^+$ cross section with the cross sections for the $\Sigma^- - K^+$ and $\Sigma^\circ - K^\circ$ productions (reactions 1 and 2 in the INTRODUCTION), there are certain relationships which follow from the assumption that the production interactions are charge-independent. The isotopic spin wave functions for the $\Sigma - K$ combinations are the same as those for the pion-nucleon combinations. The total isotopic spin can have two values $T = 3/2$ and $T = 1/2$ and, since we assume that $\vec{T}$ is a constant of the motion, there are only two production amplitudes -- $A(\frac{3}{2})$ and $A(\frac{1}{2})$ -- which are needed to describe all the possible $\Sigma - K$ productions from pion-nucleon interactions; provided, of course, that the incident pion-nucleon system is unpolarized. The situation is, thus, entirely analogous to that for pion-nucleon scattering described in reference 13.

The isotopic spin wave functions necessary to describe the reactions 1, 2 and 3 are

$$(\pi^-,p) = (\Sigma^-,K^+) = \sqrt{1/3}\left|\tfrac{3}{2},-\tfrac{1}{2}\right\rangle + \sqrt{2/3}\left|\tfrac{1}{2},-\tfrac{1}{2}\right\rangle \qquad \text{(V-1)}$$

$$(\Sigma^\circ,K^\circ) = \sqrt{2/3}\left|\tfrac{3}{2},-\tfrac{1}{2}\right\rangle - \sqrt{1/3}\left|\tfrac{1}{2},-\tfrac{1}{2}\right\rangle \qquad \text{(V-2)}$$

$$(\pi^+,p) = (\Sigma^+,K^+) = \left|\tfrac{3}{2},\tfrac{3}{2}\right\rangle \qquad \text{(V-3)}$$

with the usual notation that an eigenfunction corresponding to quantum numbers T and T_z is written as $|T,T_z\rangle$. In the $\pi^- - p$ case, the outgoing wave function will be given by

$$\psi^- = \sqrt{1/3}\, A(\tfrac{3}{2})\left|\tfrac{3}{2},-\tfrac{1}{2}\right\rangle + \sqrt{2/3}\, A(\tfrac{1}{2})\left|\tfrac{1}{2},-\tfrac{1}{2}\right\rangle \qquad \text{(V-4)}$$

and in the π^+ - p case it is just

$$\psi^+ = A(\tfrac{3}{2})\left|\tfrac{3}{2},\tfrac{3}{2}\right\rangle \qquad \text{(V-5)}$$

Solving equations (V-1), (V-2) and (V-3) for $\left|\tfrac{3}{2},-\tfrac{1}{2}\right\rangle$, $\left|\tfrac{1}{2},-\tfrac{1}{2}\right\rangle$ and $\left|\tfrac{3}{2},\tfrac{3}{2}\right\rangle$ and substituting in equations (V-4) and (V-5) we obtain

$$\psi^- = 1/3\ [A(\tfrac{3}{2}) + 2A(\tfrac{1}{2})]\ (\Sigma^-,K^+) + \frac{\sqrt{2}}{3}\ [A(\tfrac{3}{2}) - A(\tfrac{1}{2})]\ (\Sigma^\circ,K^\circ) \qquad \text{(V-6)}$$

$$\psi^+ = [A(\tfrac{3}{2})]\ (\Sigma^+,K^+) \qquad \text{(V-7)}$$

The observable production amplitudes, expressed in terms of the T = 3/2 and T = 1/2 production amplitudes are therefore[13]

$$\left\langle \pi^+ p \middle| \Sigma^+ K^+ \right\rangle = A(\tfrac{3}{2}) \qquad \text{(V-8)}$$

$$\left\langle \pi^- p \middle| \Sigma^- K^+ \right\rangle = 1/3\ [A(\tfrac{3}{2}) + 2A(\tfrac{1}{2})] \qquad \text{(V-9)}$$

$$\left\langle \pi^- p \middle| \Sigma^\circ K^\circ \right\rangle = \frac{\sqrt{2}}{3}\ [A(\tfrac{3}{2}) - A(\tfrac{1}{2})] \qquad \text{(V-10)}$$

and the cross sections for the processes are given by

$$\sigma(+) = \left| \left\langle \pi^+ p \middle| \Sigma^+ K^+ \right\rangle \right|^2 \quad \text{etc.} \qquad \text{(V-11)}$$

For any two complex numbers Z_1 and Z_2 we have

$$|Z_1| + |Z_2| \geq |Z_1 + Z_2| \geq \left| |Z_1| - |Z_2| \right| \qquad \text{(V-12)}$$

Thus, putting

$$Z_1 \equiv \left\langle \pi^- p \middle| \Sigma^- K^+ \right\rangle \qquad \text{(V-13)}$$

$$Z_2 \equiv \sqrt{2}\ \left\langle \pi^- p \middle| \Sigma^\circ K^\circ \right\rangle \qquad \text{(V-14)}$$

we obtain

$$\sqrt{\sigma(-)} + \sqrt{2\sigma(o)} \geq \sqrt{\sigma(+)} \geq \left| \sqrt{\sigma(-)} - \sqrt{2\sigma(o)} \right| \qquad \text{(V-15)}$$

The above inequalities are equivalent to Feldman's triangular relationships[14] which, in effect, state that three vectors of magnitude $\sqrt{\sigma(+)}$, $\sqrt{2\sigma(o)}$ and $\sqrt{\sigma(-)}$ must be able to be made into a triangle--if charge independence is to hold.

A comparison of the $\Sigma^+ - K^+$ total cross section with those for the $\Sigma^- - K^+$ and $\Sigma^\circ - K^\circ$ reactions[15], which were obtained in the same chamber and at the same energy, shows that the triangular relationships are satisfied since the three cross sections are about equal. In the case of the differential cross sections, that of the $\Sigma^- - K^+$ is peaked forward like the $\Sigma^+ - K^+$ but the $\Sigma^\circ - K^\circ$ is peaked backward. Thus, in the quadrant for sigma center-of-mass production angles between 120° and 180° the triangular relationships cannot be satisfied, indicating a violation of charge independence.

A more detailed discussion of these consequences and the possible errors involved can be found in reference (16). Further experiments now in progress at the Cosmotron and Bevatron should help to clarify the question.

VI. LIFETIME OF THE Σ^+

In all nineteen identified hydrogen productions, the Σ^+ decayed in the chamber. There were no cases which were recognized on the basis of the K^+ decay alone. Since the momentum of the Σ^+ is determined by the reaction kinematics, it is possible to calculate the time t_{cm} that each Σ^+ lived in its own center-of-mass system before decaying. The relationship is is

$$t_{cm} = \frac{M}{c} \cdot \frac{l}{p} \qquad \text{(VI-1)}$$

where p is the Σ^+ momentum in Bev/c, l is its path length in cemtimeters and c is the velocity of light. The Σ^+ mass, M, was taken as 1.189 Bev. Using this same formula the potential lifetime T_{cm} for each Σ^+ can also be determined from its potential path L. By potential path is meant the distance the particle would have traveled, had it not decayed, before leaving the observable volume of the bubble chamber. The observable volume was taken to be 0.5 cm smaller in every dimension than the physical volume, this being the approximate distance needed to observe a decay.

A maximum likelihood technique was used to estimate the mean lifetime τ for the Σ^+ giving the best fit to our data. The form of the likelihood function is due to Bartlett[17]. It is given by

$$L(\tau) = \prod_{i=1}^{19} \frac{\tau^{-1} \exp[-(t_{cm})_i/\tau]\, dt_i}{1 - \exp[-(T_{cm})_i/\tau]} \qquad \text{(VI-2)}$$

which is proportional to the probability, as a function of τ, of obtaining the observed data. The fact that the chamber is finite in size means that it is possible for sigmas to leave the chamber before decaying and thus leave

their production reaction undetected. This is accounted for by the denominator of the likelihood function, which is supposed to be the probability of observing the i^{th} particle decay. The time T_{cm} should therefore be calculated from a space interval over which the decay detection efficiency is 100%, or at least constant and the same for all particles. Since the Σ^+ lifetime is short, there was reason to believe that there would be an appreciable number of them which were missed by the scanners due to their short path length. If not taken into account, this effect would tend to make our estimate of the Σ^+ lifetime too large. In order to investigate this question, the frequency of events vs. the Σ^+ path length l was plotted and is shown in Figure 8. For this purpose, the real $\Sigma^+ - K^+$ events were not used since they might show a preference for short lengths because of their exponental decay law. Thus, we have considered here all the measured pseudo-sigmas, most of which are double scatterings, with l being the distance between the first and second scattering. The frequency of double scatterings also follows an exponental law, but the mean path is so large that the effect can be neglected. The detection efficiency seems to be constant for values of l between 0.4 cm and 5 cm, but there is a definite cut-off below 0.4 cm. Putting this fact into the likelihood function, it would read

$$L(\tau) = \prod_{i=1}^{19} \frac{\tau^{-1} \exp\left[-(t_{cm})_i/\tau\right] dt_i}{\exp\left[-(t_o)_i/\tau\right] - \exp\left[-(T_{cm})_i/\tau\right]} \qquad \text{(VI-3)}$$

the times $(t_o)_i$ being calculated from the relation

$$(t_o)_i = \frac{M}{c} \frac{l_o}{p_i} \qquad \text{(VI-4)}$$

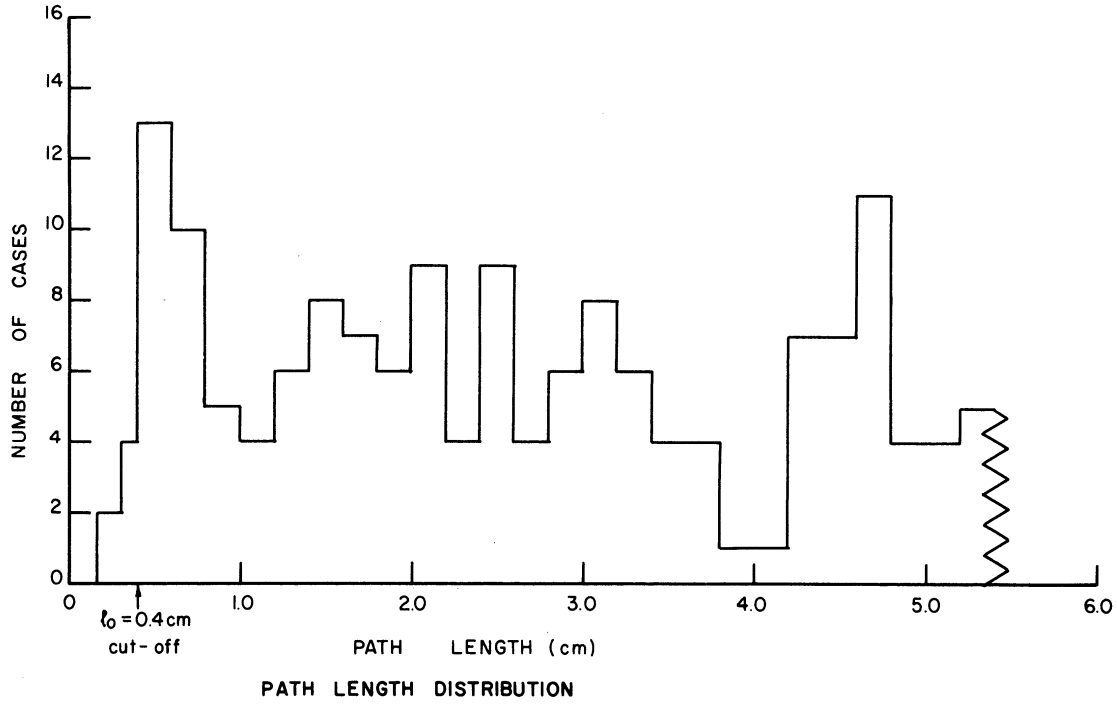
NUMBER OF CASES
16
14
12
10
8
6
4
2
0
0
1.0
2.0
3.0
4.0
5.0
6.0
ℓ_0 = 0.4 cm
cut-off
PATH LENGTH (cm)
PATH LENGTH DISTRIBUTION

FIGURE 8

with $l_o \equiv 0.4$ cm. Putting $t_i = (t_{cm})_i - (t_o)_i$ and $T_i = (T_{cm})_i - (t_o)_i$, we obtain the likelihood function which was used:

$$L(\tau) \equiv \prod_{i=1}^{19} \frac{\tau^{-1} \exp\left[-t_i/\tau\right] dt_i}{1 - \exp\left[-T_i/\tau\right]} \qquad \text{(VI-5)}$$

This differs from the definition (VI-2) only in that the origin for the times t_{cm} and T_{cm} is chosen as the point beyond which the detection effici-efficiency is constant.

A list of the data pertinent to the lifetime calculation is given in Table II on the following page.

The likelihood function (VI-5) is plotted in Figure 9. The value obtained for the Σ^+ mean lifetime is

$$\tau = 0.95^{+\ 0.37}_{-\ 0.23} \times 10^{-10} \text{ sec.}$$

The errors come from the width of the curve at half maximum. This is in good agreement with the various emulsion results although the California hydrogen bubble chamber results are somewhat lower. Besides the quoted errors, which are due to the small number of observations, there is also the possibility of error arising from the measurement of the Σ^+ momentum and path lengths. Excluding any systematic errors, these are quite small and of a random nature and, thus, will be insignificant in comparison with the quoted errors. A possible source of systematic error would be that the scanning bias against short path lengths was much worse than that which we have already taken into account. This would tend to make our present estimate of τ too large.

TABLE II. Σ^+ LIFETIME DATA

Event Number	Σ^+ Momentum (Bev/c)	$t_i (10^{-10}$ sec)	$T_i (10^{-10}$ sec)
68696	1.11	1.35	7.69
70539	1.00	0.60	7.24
70595	0.76	0.23	12.19
74866	1.16	0.12	5.69
76281	0.93	0.62	2.39
78476	0.89	0.22	5.19
78481	0.96	1.08	3.27
79426	1.06	0.01	6.09
81602	1.04	0.04	3.67
82509	0.98	2.48	6.60
83328	1.00	1.12	10.70
83391	0.85	0.29	2.90
86910	0.85	1.16	10.25
86759	1.11	1.54	8.31
86317	1.04	1.73	4.37
69905	1.09	0.68	3.10
82967	1.03	0.41	9.67
72295	1.02	2.75	6.73

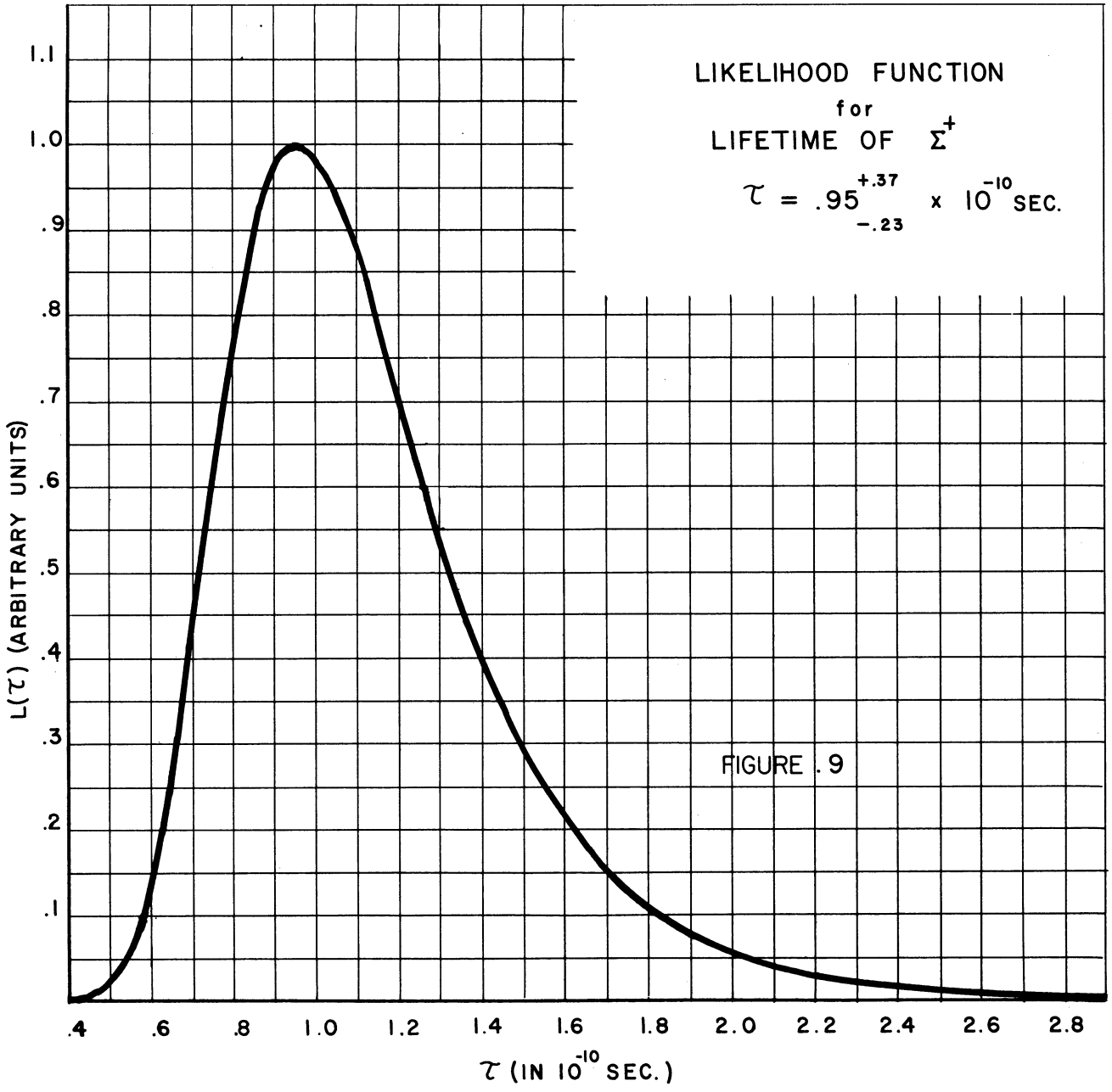
LIKELIHOOD FUNCTION
for
LIFETIME OF Σ^+
$\tau = .95^{+.37}_{-.23} \times 10^{-10}$ SEC.
L(τ) (ARBITRARY UNITS)
1.1
1.0
.9
.8
.7
.6
.5
.4
.3
.2
.1
.4
.6
.8
1.0
1.2
1.4
1.6
1.8
2.0
2.2
2.4
2.6
2.8
τ (IN 10^{-10} SEC.)

FIGURE . 9

There was no evidence for the existence of two types of Σ^+ hyperons exhibiting two different lifetimes, as might be expected if the Σ^+ had a parity doublet structure[18]. However, due to small number of events, such a double lifetime could easily escape detection; especially if the two values did not differ greatly. On the other hand, if there were extremely long-lived sigmas ($\tau > 5 \times 10^{-9}$ sec) being produced in numbers comparable to the above cases, they would, in all probability, escape the chamber and thus go undetected. A similar situation would obtain for an extremely short-lived counterpart ($\tau < 0.1 \times 10^{-10}$ sec). In this case, practically all of them would decay before going 0.4 cm, which would be too short for efficient scanning. The evidence against these possibilities is that in no case where a stopping K meson was identified did the associated particle fail to show a decay. Of course, this fact also lends support to the hypothesis of associated production.

VII. DECAY ANGULAR DISTRIBUTIONS

It has been suggested by several authors that by looking at the angular distributions of products from decaying hyperons one might expect to gain information regarding the following questions:

1. Is parity not conserved in the decay?[19]
2. Does the hyperon exist as two distinct particles which are related to each other by parity conjugation?[19]
3. Is the spin of the hyperon greater than 1/2?

In our particular process there is, in each case, a production plane defined as well as the direction of the Σ^+ line of flight. Thus, it is possible to unambiguously define a three-dimensional coordinate system and study the distributions in both the azimuthal angle Φ, and the polar angle Θ of the decay.

Being fully aware that angular distributions involving such a small number of events cannot be very meaningful, we nevertheless present the pertinent data which may be of interest.

First of all, let us describe the coordinate system to be used in the following discussion. Referring to Figure 10, the z axis is taken to be in the direction of flight of Σ^+. The plane formed by the direction $\vec{p}_{inc}$ of the incoming π^+ meson and that of the emergent hyperon, $\vec{p}_{\Sigma}$, is the production plane. We then take the y axis as perpendicular to this plane. To be specific, $y \equiv \vec{p}_{inc} \times \vec{p}_{\Sigma}$. The x axis is then given by $\vec{x} \equiv \vec{y} \times \vec{z}$ in the usual manner for a right-handed coordinate system. We denote the direction of the π^+ or π° meson arising from the decay by the usual spherical polar angle Θ and azimuthal angle Φ in this system. The origin is assumed to coincide with the center-of mass of the Σ^+.

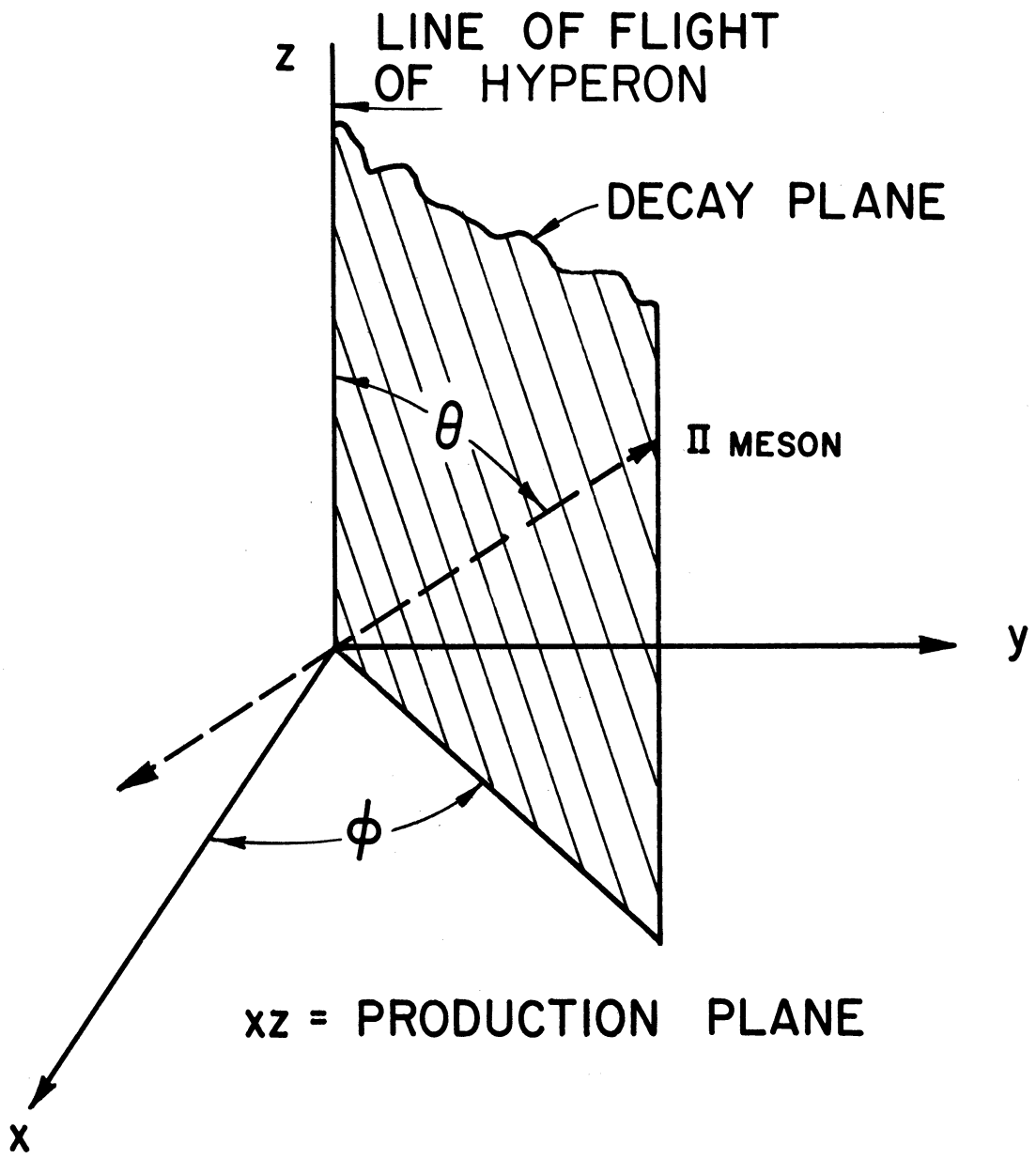

FIGURE 10

COORDINATE SYSTEM

1. Parity non-conservation: In this case, the relevant distribution[20] is that of the azimuthal angle in the range 0° to 360° which is shown in Figure 11. Any asymmetry (about 180°) in this distribution would mean that parity is not conserved in the Σ^+ decay.

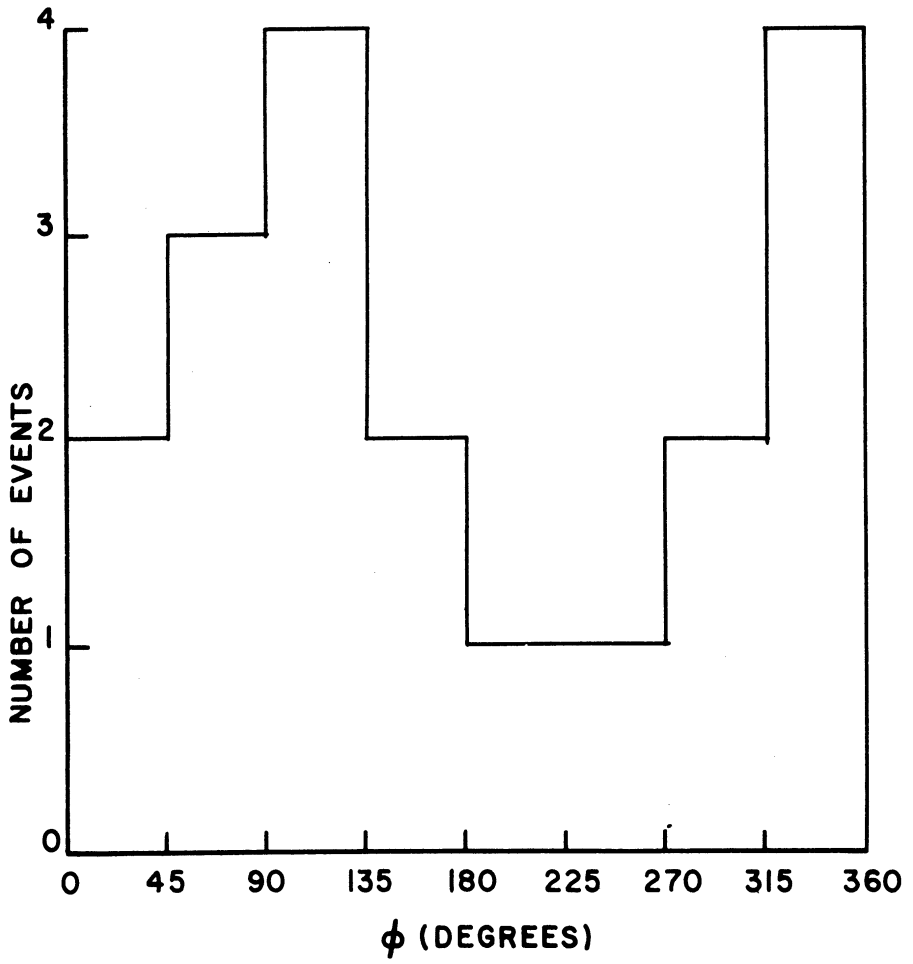

Σ^+ AZIMUTHAL ANGULAR DISTRIBUTION FOR DECAY

FIGURE II

2. Parity doublets: To test this hypothesis one should look at both the θ and the once-folded φ distributions. When by the latter we mean the distribution shown in Figure 11 folded about 180° so that the angles φ and $2\pi - \varphi$ ($0° \leqq \varphi \leqq 180°$) are considered equivalent. The resulting distributions are shown in Figure 12. Any possible real asymmetry due to the non-conservation of parity would be washed out in the folding process and we are left in a situation similar to case 1. An asymmetry (about 90°) in either of these distributions would be proof that parity doublets exist for the Σ^+.

3. Spin: The pertinent distributions in this case are obtained by folding those shown in Figure 12 about 90° in a manner similar to that described above. The results are shown in Figure 13. This operation washes out any effects due to the possible existence of parity doublets or parity non-conservation. A deviation from <u>isotropy</u> in either of these distributions would mean that the spin of the Σ^+ was greater than 1/2.

Of course, all these effects depend for their existence upon the Σ^+ being polarized in the production process, about which very little is known. Moreover, even in the case of a substantial polarization the effects might be small.

We feel that there is nothing in any of these distributions to warrant any conclusions, favorable or unfavorable, towards parity conservation, parity doublets, or high spin for the Σ^+.

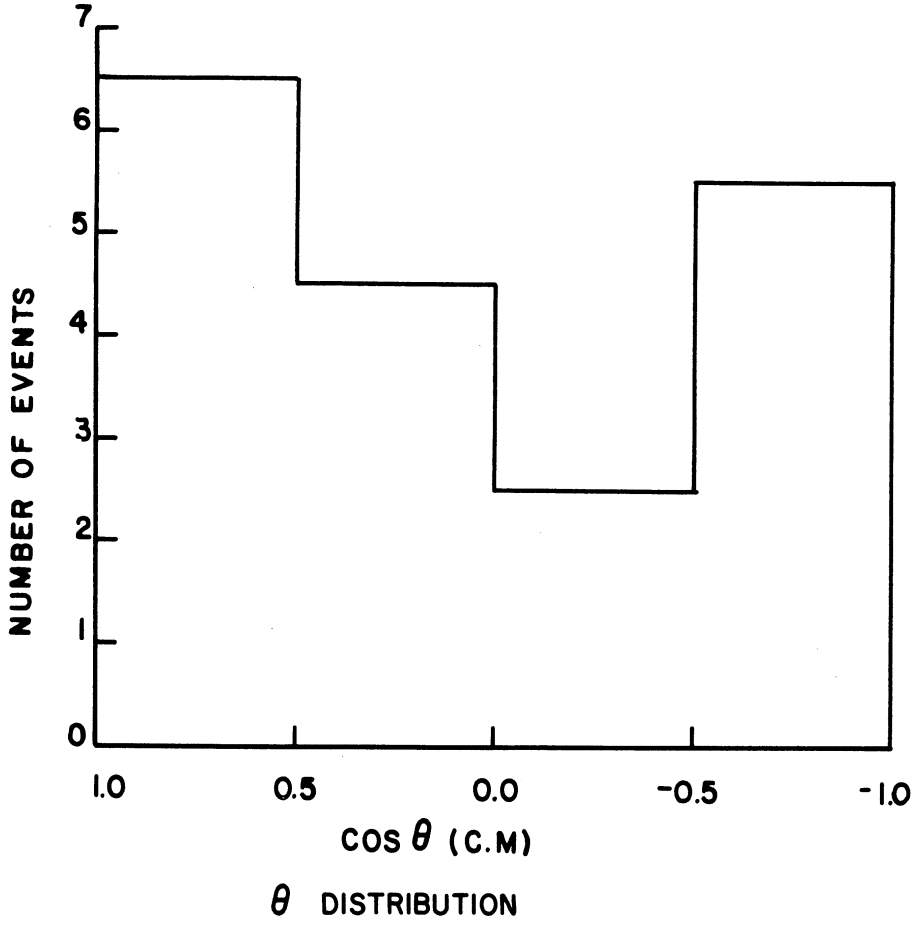

θ DISTRIBUTION

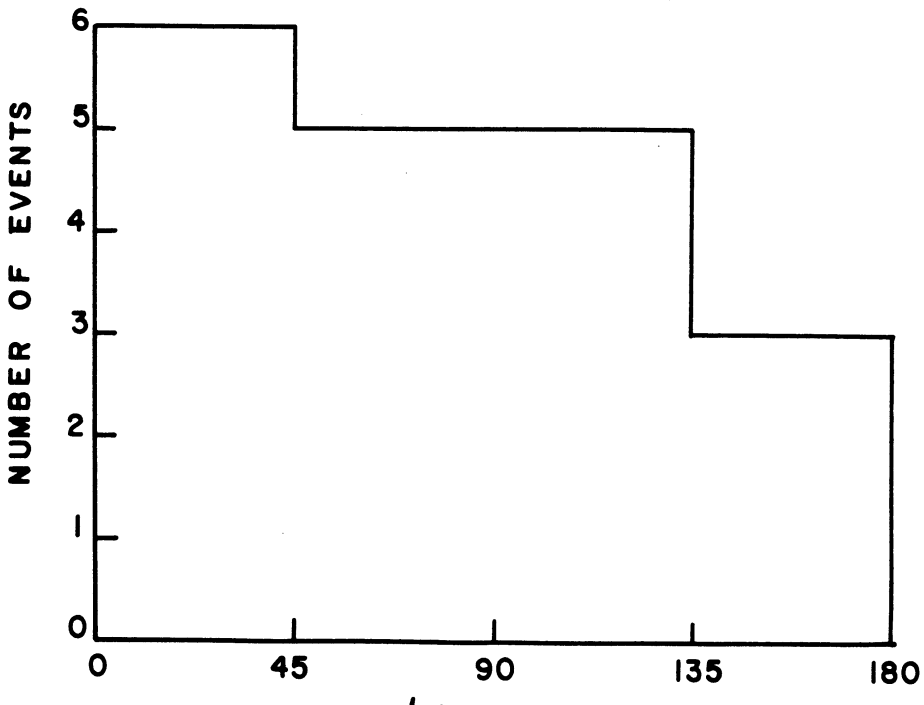

ONCE-FOLDED φ DISTRIBUTION

FIGURE 12

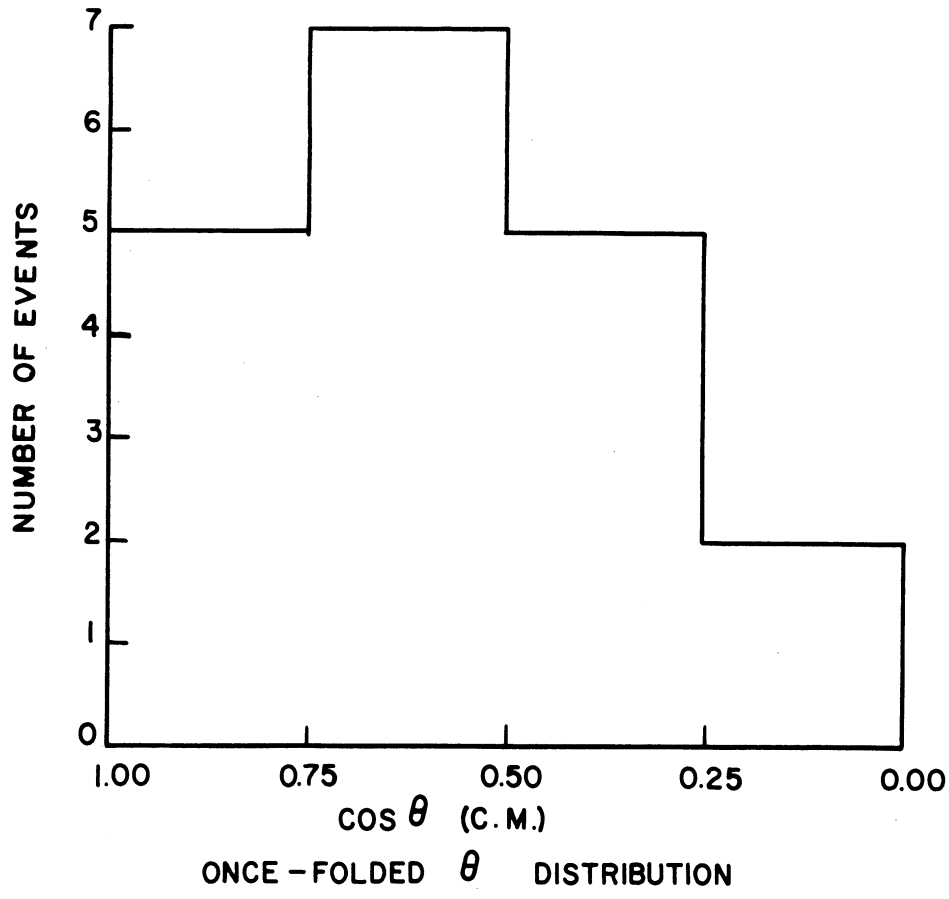
NUMBER OF EVENTS
0
1
2
3
4
5
6
7
1.00
0.75
0.50
0.25
0.00
COS θ (C.M.)
ONCE-FOLDED θ DISTRIBUTION

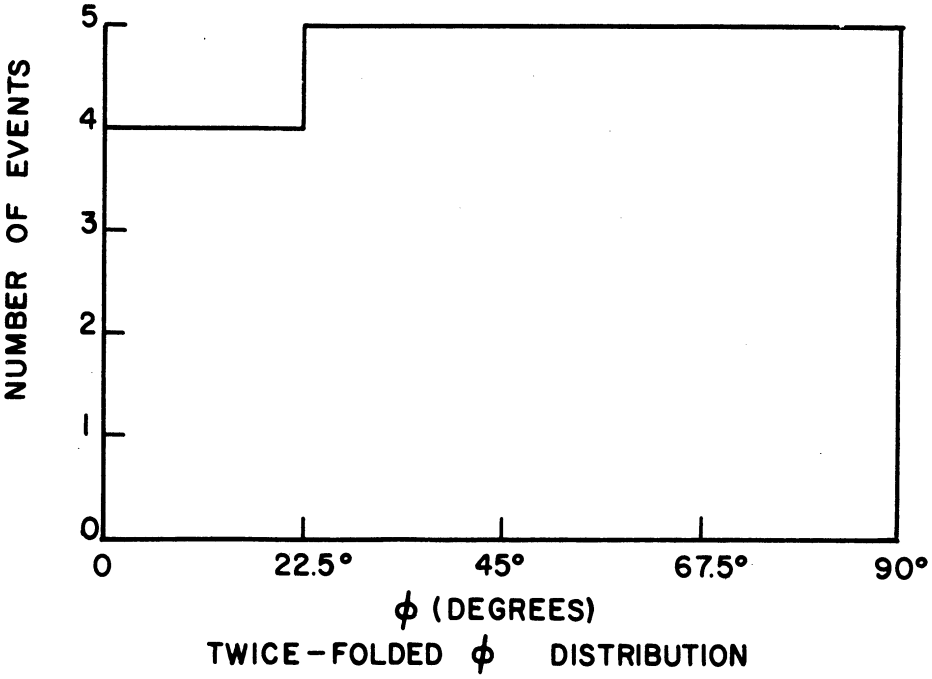
NUMBER OF EVENTS
0
1
2
3
4
5
0
22.5°
45°
67.5°
90°
φ (DEGREES)
TWICE-FOLDED φ DISTRIBUTION

FIGURE 13

VIII. CONCLUSION

This experiment has shown the feasibility of performing bubble chamber experiments in high energy positive pion beams of the quality that can be obtained from the Cosmotron. In particular, the reaction $\pi^+ + p \rightarrow \Sigma^+ + K^+$ was studied. It was found that the hyperons from these reactions apparently have the same properties as those from the more familiar reaction $K^- + p \rightarrow \Sigma^+ + \pi^-$.

The total cross section for the process $\pi^+ + p \rightarrow \Sigma^+ + K^+$ is about the same as for the reactions $\pi^- + p \rightarrow \Sigma^- + K^+$ and $\pi^- + p \rightarrow \Sigma^\circ + K^\circ$. The fact that the $\Sigma^+ - K^+$ reaction occurs at all means that the $T = 3/2$ state of the pion-nucleon system surely participates in strange particle productions. Moreover, the fact that the three cross sections are of about the same size indicates that the $T = 1/2$ state also participates; since if it were all $T = 3/2$, the ratios of the cross sections would be[13] $\sigma(+) : \sigma(-) : \sigma(o) = 9:1:2$ which certainly seems to be outside experimental error.

The fact that our data on the <u>differential</u> cross sections is inconsistent with the hypothesis of charge independence points to a more thorough study of the reactions in question.

IX. BIBLIOGRAPHY

1. Rochester, G. D. and Butler, C. C., Nature 160, 855 (1947).
2. Gell-Mann, M., Phys. Rev. 92, 833 (1953).
3. Nakano, T. and Nishijima, K., Prog. Theor. Phys. 10, 581 (1953).
4. Cool, Piccioni and Clark, Phys. Rev. 103, 1082 (1956).
5. Abashian, Cool, Cronin and Piccioni (unpublished data).
6. Brookhaven National Lab. Report CCD-1.
7. Brookhaven National Lab. Report RMS-55.
8. Rossi, B., High Energy Particles, Prentice-Hall, New York, 67 (1952).
9. Rahm, D. C., Bull. Am. Phys. Soc., Ser. II-2, No. 1, 11 (1957).
10. Cool, Piccioni and Clark, Phys. Rev. 103, 1082 (1956).
11. Glaser, Rahm and Dodd, Phys. Rev. 102, 1653 (1956).
12. Wattenberg, A., et al., Phys. Rev. (to be published).
13. Bethe, H. A. and de Hoffmann, F., Mesons and Fields, Row, Peterson and Company, New York, 62 (1955).
14. Feldman, D., Phys. Rev. 103, 254 (1956).
15. Brown, J. L., Glaser, D. A., and Perl, M. L., Phys. Rev. (to be published).
16. Brown, J. L., et al., Phys. Rev. 107, 906 (1957).
17. Bartlett, M. S., Phil. Mag. 44, 249 (1953).
18. Lee, T. D. and Yang, C. N., Phys. Rev. 102, 290 (1956).
19. Lee, T. D. and Yang, C. N., Phys. Rev. 104, 822, 254 (1956).
20. Morpurgo, G., Nuovo Cimento IV, N. 5, 1222 (1956).